CALIFORNIA STATE POLYTECHNIC UNIVERSITY POMONA

AEROSPACE ENGINEERING DEPARTMENT

SHARP

SUBSONIC HIGH ALTITUDE RESEARCH PLATFORM

Team Members:
Todd Beals
Craig Burton
Aileen Cabatan
Christine Hermano
Tom Jones
Susan Lee
Brian Radloff

Professor:
Paul A. Lord

Dedicated to our friend,

Russell E. Bell,

with love and support.

ABSTRACT

At the equator, the ozone layer ranges from 65,000 to 130,000+ ft which is beyond the capabilities of the ER-2, NASA's current high altitude reconnaissance aircraft. The Universities Space Research Association, in cooperation with NASA, is sponsoring an undergraduate program which is geared to designing an aircraft that can study the ozone layer at the equator. This aircraft must be able to satisfy four mission profiles. Mission One is a polar mission which ranges from Chile to the South Pole and back to Chile, a total range of 6000 n.mi. at 100,000 ft with a 2500 lb payload. The second mission is also a polar mission with a decreased altitude of 70,000 ft and an increased payload of 4000 lbs. For the third mission, the aircraft will take-off at NASA Ames, cruise at 100,000 ft carrying a 2500 lb payload, and land in Puerto Montt, Chile. The final mission requires the aircraft to take-off at NASA Ames, cruise at 100,000 ft with a 1000 lb payload, make an excursion to 120,000 ft, and land at Howard AFB, Panama. All three missions require that a subsonic Mach number be maintained due to constraints imposed by the air sampling equipment. The aircraft need not be manned for all four missions. Three aircraft configurations have been determined to be the most suitable for meeting the above requirements. In the event that a requirement can not be obtained within the given constraints, recommendations for proposal modifications are given.

TABLE OF CONTENTS

TABLE OF CONTENTS (Continued)

TABLE OF CONTENTS (Continued)

NOMENCLATURE

SYMBOLS

Al	Aluminum
Bo	Boron
C_d	Section drag coefficient
C_l	Section lift coefficient
D	Drag
Ep	Epoxy
Gr	Graphite
L	Lift
R	Rankine
S_{ref}	Wing planform area
Ti	Titanium
V	Velocity
a	Aileron
b	Wing span
c	Mean geometric chord
e	Elevator
n	Load Factor
r	Rudder

GREEK SYMBOLS

ω	Frequency
θ	Pitch angle
ζ	Damping ratio

ACRONYMS

AAOE	Airborne Antarctic Ozone Experiment
AASE	Airborne Arctic Stratosphere Expedition
AC	Alternating current
BFL	Balanced field length
CFC	Chlorofluorocarbon
c.g.	Center of gravity
DC	Direct current
FAA	Federal Aviation Administration
FAR	Federal Aviation Regulations
LCC	Life cycle cost
NACA	National Advisory Committee on Aeronautics
NASA	National Aeronautics and Space Administration
O_2	Oxygen
RTD&E	Research, test, development and evaluation
RFP	Request for proposal

NOMENCLATURE (Continued)

SFC	Specific fuel consumption
SHARP	Subsonic High Altitude Research Platform
TCAS	Terminal collision avoidance system
USRA	Universities Space Research Association

LIST OF FIGURES

LIST OF FIGURES (Continued)

LIST OF TABLES

1.0 INTRODUCTION

1.1 ATMOSPHERE

The most common way to describe the Earth's atmosphere is by dividing it into regions by the temperature distributions (Figure 1.1.1). The lowest region in this system is the troposphere. This is a region of constant turbulence and mixing. This constant turbulence

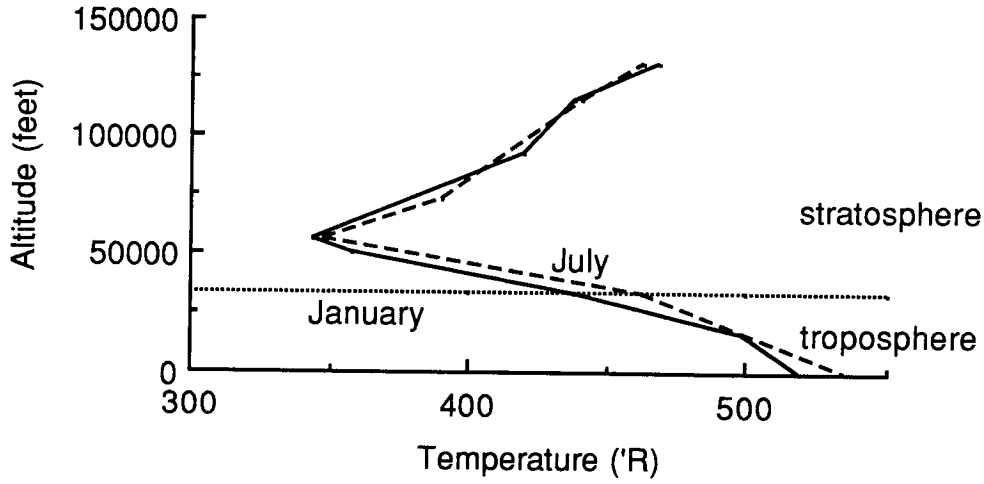

Figure 1.1.1 Temperature profile at the equator

drives weather across the hemispheres and keeps the composition in this region uniform. The temperature is this region decreases almost linearly due to the increasing distance from the sun warmed Earth. Right above this is the stratosphere. Temperature in this region stops falling and remains constant and then increases again. At one point, it was believed that the stratosphere had no turbulence. Scientists now know that the stratosphere is a region of extremely strong jet streams. This also causes this region to have a generally uniform composition with the exception of one chemical concentration, ozone. The concentration

of ozone from the troposphere to the middle of the stratosphere changes from 0.4 parts per million to 10 parts per million. Most of all the ozone that is created remains in this region. Throughout these region, the density almost constantly decreases exponentially. By the time an altitude of 100,000 ft is reached, the density decreases to 1/100 of that at sea level (Figure 1.1.2). This is a main design driver and

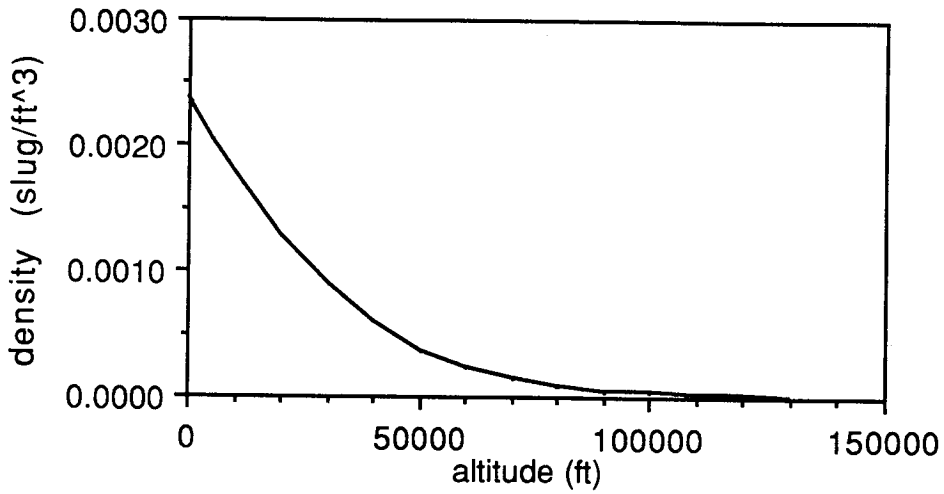

Figure 1.1.2 Density variation

seriously affects the propulsion of the aircraft.

Winds and turbulence are a very important factor of atmospheric conditions. Some sources of turbulence are thunderstorms, wind shear, jet streams, convection due to morning warming of air close to the ground, or any weather patterns.Global circulation is known as the larger scale wind patterns permanent features of the atmosphere. There are continuous streams of air from the poles to the equators at

the low altitudes and streams from the equator to the poles at the high altitudes. These air masses are distorted by the rotation of the Earth and generate prevailing winds. This plus the rising air warmed by the Earth's surface and colder air rushing down to replace it cause the constant churning in the troposphere. Recent wind profiles over Florida in October 1989 and February 1990 are shown in Figure 1.1.3 .

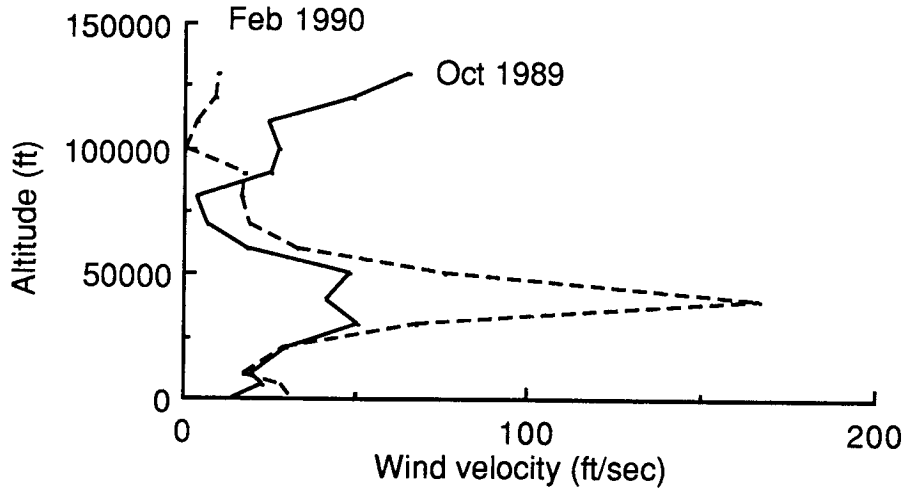

Figure 1.1.3 Wind profile comparison

1.2 OZONE

Stratospheric ozone protects all forms of life on earth by creating a barrier that prevents the sun's ultraviolet radiation from entering the Earth's atmosphere. Ozone is produced when solar ultraviolet rays bombard ordinary oxygen molecules (O_2) existing in the atmosphere and break them down. These free oxygen atoms recombine with O_2 to form ozone, another form of oxygen. This form of oxygen is able to absorb ultraviolet light. Most ozone is formed in the stratosphere and in this way protects oxygen in the lower altitudes from

being broken up and keeps most ultraviolet rays from penetrating to the Earth's surface. The ozone layer is located 35,000 to 95,000 ft over the poles, 50,000 to 100,000 ft over the mid-latitudes and 65,000 to 125,000 ft over the tropics.

Scientists with the British Antarctic Survey were the first to observe that ozone concentrations in the stratosphere were dropping at dramatic rates over Antarctica each southern spring (and being gradually replenished by the end of the November). Currently, similar trends of ozone destruction have been discovered over the Arctic at much lesser degrees than over the Antarctic. Analysis of data also show that long-term decreases in ozone that have been occurring in the mid- to high latitudes in the Northern hemisphere during winters for the past few decades.

Scientists have since then discovered and widely accepted that winds are partly responsible. But that the major contributing factor of the ozone depletion is due to chlorofluorocarbons or CFC's. CFC's can be found everywhere - in coolants of refrigerators and air conditioners, used to make plastic foam and cleaning solvents. CFC's rise form the earth into the stratosphere where it sets off chemical reactions that destroy ozone.

1.3 DESIGN SUMMARY

Recent discoveries of ozone depletion in the Earth's atmosphere have initiated the need for detailed chemical analysis studies to be performed in the levels of the atmosphere which contain ozone. These studies require careful sampling and analysis of the

atmosphere which must be performed subsonically and at altitudes ranging from 80,000 to 100,000+ ft. In cooperation with NASA/USRA, the Cal Poly, Pomona design team has developed the unmanned Subsonic, High-Altitude Research Platform (**SHARP**) to satisfy this demand.

The **SHARP** is a long-range, joined-wing aircraft which is virtually independent of any ground or vehicle support. The aircraft is capable of meeting or exceeding all of the mission requirements with the exception of altitude jumping. The finalized design allows for a wide range of flexibilities from supporting various instrumentation packages and payloads to rapid and easy conversion to a manned operational mode. The airframe, skins, and propellers will be constructed of 100% composite materials for weight savings, increased structural integrity, and overall improved performance. The aircraft will be self propelled and runway launched by three internal combustion engine/propeller combinations with three stages of turbocharging. The configuration and engine placement ease the maintainability of the aircraft.

2.0 MISSION REQUIREMENTS AND OBJECTIVES

The goal in designing this aircraft is to carry large, multi-instrument payloads to any spot on the globe in any season. Some of the key specifications are shown below:

Destination:	•Any point on the globe •South Pole •Midlatitudes
Cruising Altitude:	•100,000 ft •Depending on mission, this altitude may vary +/- 30,000 ft actual altitude must not be maintained constantly; slight variation is possible as long as noted.
Speed:	•Subsonic; M=0.6, variable down to M=0.4 to test experimental inlet losses.
Range:	•Total = 6000 nautical miles •Cruise = 5000 n. mi.
Operational Mode:	•Unmanned and manned •Day and night polar flights •Unrestricted over oceans
Operational Capability:	•Moderate to severe turbulence •Adequate margin between stall and Mach buffet
Propulsion:	•Multiple engines
Flight Envelope:	•Greater than 15 knots
Engine Envelope:	•Greater than 20% thrust
Airport Restrictions:	•Taxiways -- 75 ft wide (towed with support vehicle) •Runways -- 150 ft wide by 6000 ft long with 4 ft high obstacles 20 ft from taxiways and runways
Takeoff and Landing:	•15 knot crosswinds •200 ft cloud ceilings •One half mile visibility •Spoilers/lift dump devices for low wing loading landing

Vibration:	•Equal to or less than the ER-2
Controls:	•Redundant when fly-by-wire
Payload:	•3000 lbs •In situ instruments: Forward-looking access to the unperturbed free air stream
Remote Sensors:	•Access to upward, downward and 360° horizontal views
Wiring:	•Accommodates rapid instrument swapping and communication between instruments and master control computer
Telemetry:	•Tracking and data relay satellite system for commands and data
Landing Gear:	•Permanent
Number Required:	•Two operational aircraft

The aircraft specifications above were originally acquired from four proposed missions. In general, both in-situ and remote measurements from a very high altitude aircraft will be required and further increases in altitude are desirable.

The mission requirements and operational considerations set many of the performance and operational considerations for the aircraft. Some of these may be slightly adjusted to achieve optimal flight conditions as long as all of the mission objectives can still be adequately achieved. The application of these parameters and recommended minor adjustments will be discussed under aircraft performance.

2.1 MISSION 1: POLAR VORTEX

This mission (Figure 2.1.1) requires flights at 100,000 ft cruise altitude from a South American base to the South Pole (a round trip of 6,000 n. mi.) and the ability to fly into the polar night and over water more than 200 n. mi. from land. The range of atmospheric constituents and state variables to be measured implies a payload capability equal to that carried in AAOE and AASE missions (2,500 lbs).

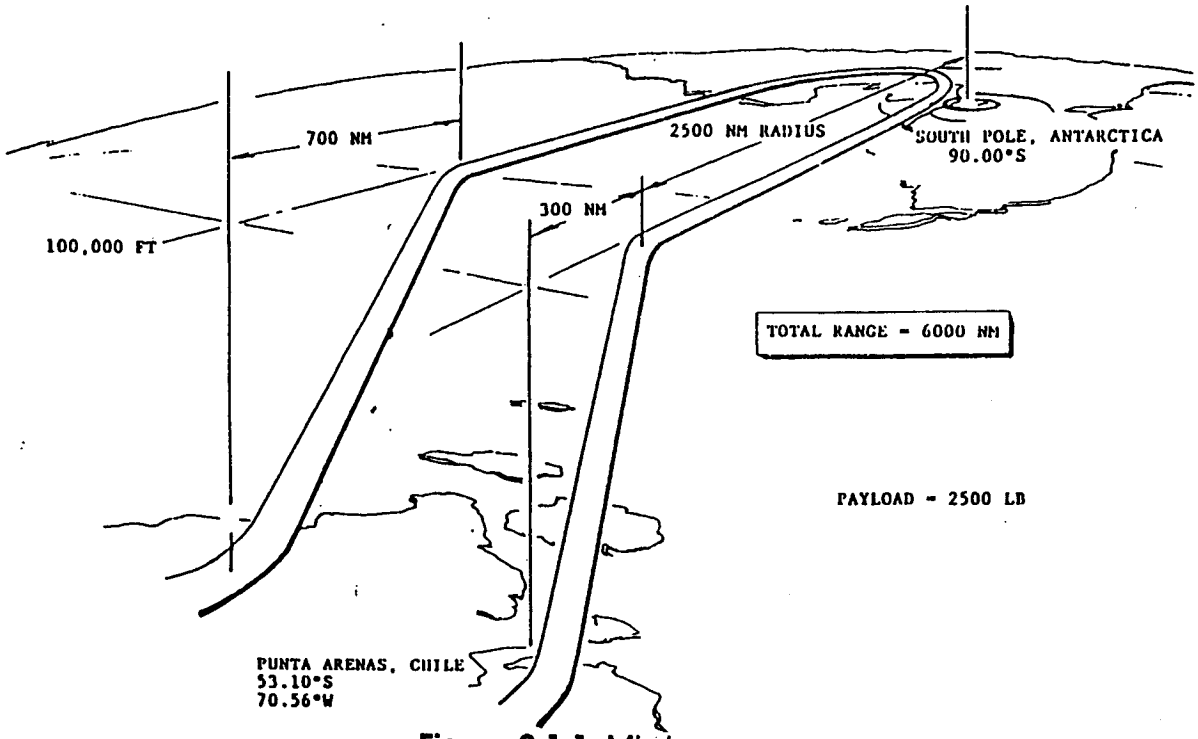

Figure 2.1.1 Mission one

2.2 MISSION 2: CHEMICAL SPECIES TRANSPORT BY GENERAL CIRCULATION

This mission (Figure 2.2.1) requires the same capabilities as Mission 1 except for a decrease in required altitude of 70,000 ft and an increase in payload to 4,000 lbs.

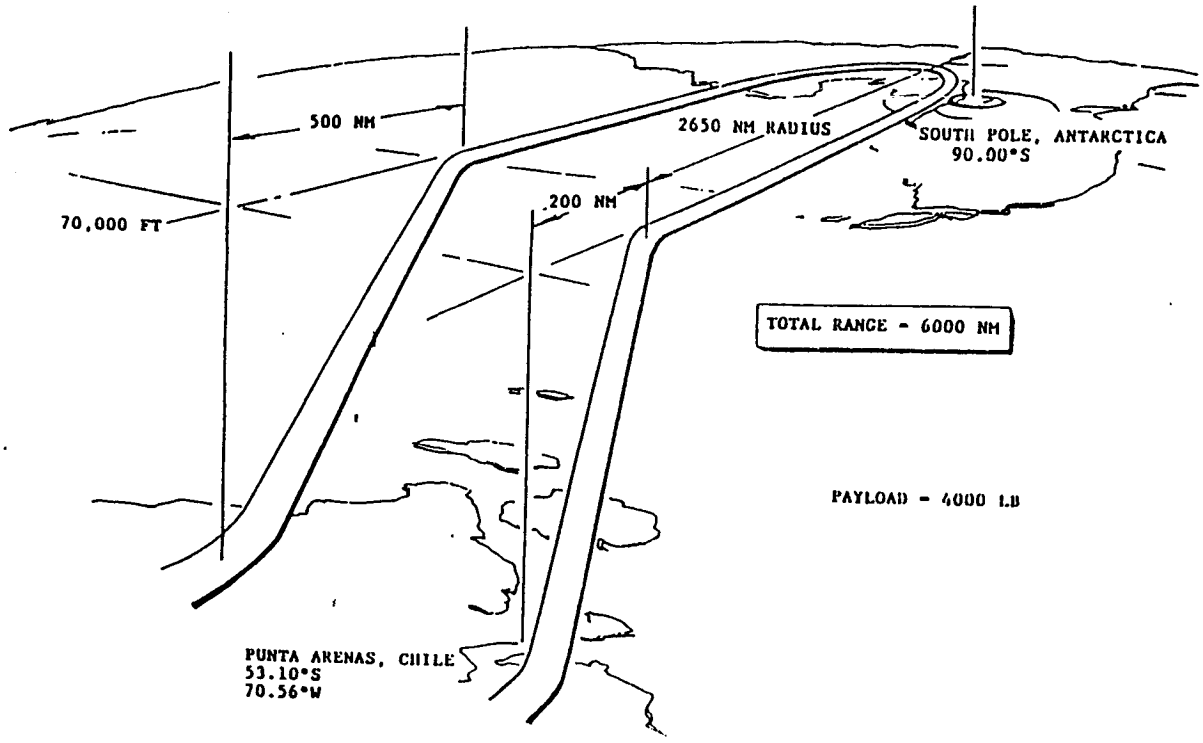

Figure 2.2.1 Mission two

2.3 MISSION 3: HIGH-ALTITUDE PHOTOCHEMISTRY IN TROPICAL AND MIDDLE LATITUDE

This mission (Figure 2.3.1) requires the ability to cruise at 100,00 ft over

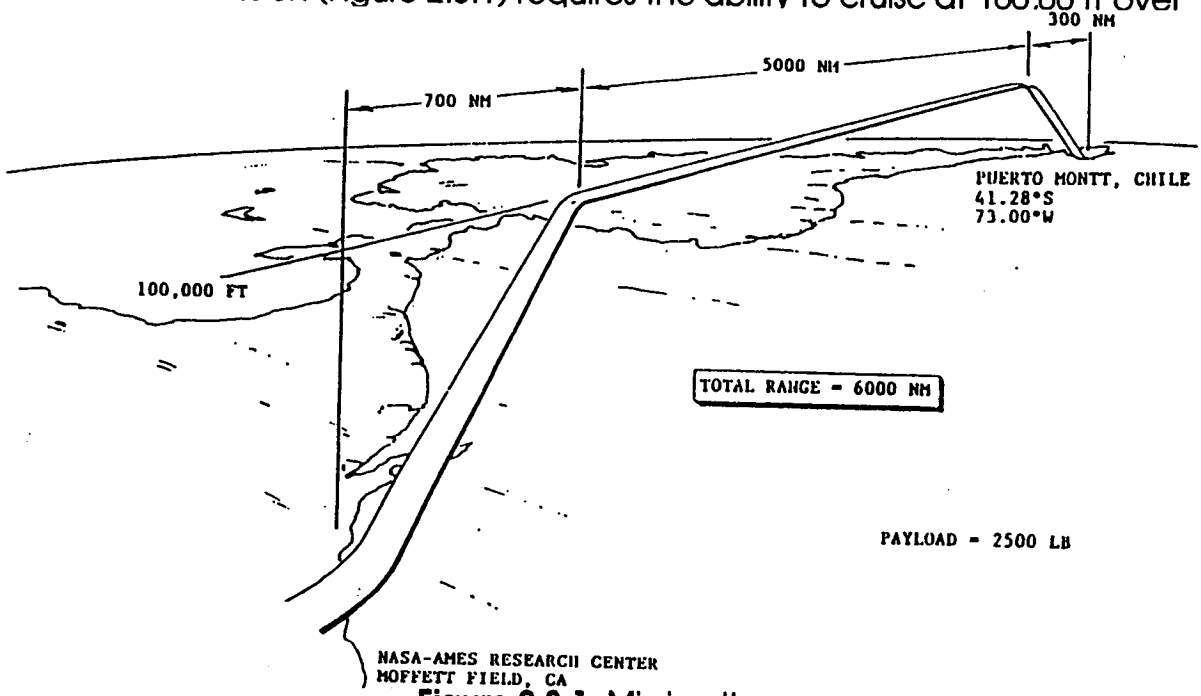

Figure 2.3.1 Mission three

wide latitude ranges (preferable from northern midlatitudes through the tropics to southern midlatitudes), or to stay aloft for a significant portion of the diurnal cycle. The ability to fly vertical profiles from cruise altitude down to about 33,000 ft, and to remain over water for long periods, is also required. The range of atmospheric constituents and state variables to be measured implies a payload capability equal to that carried in the AAOE and AASE missions (2,500 lb).

2.4 MISSION 4: VOLCANIC, STRATOSPHERIC CLOUD / AEROSOL, GREENHOUSE, AND RADIATION BALANCE STUDIES

This mission (Figure 2.4.1) requires the ability to cruise at altitudes of

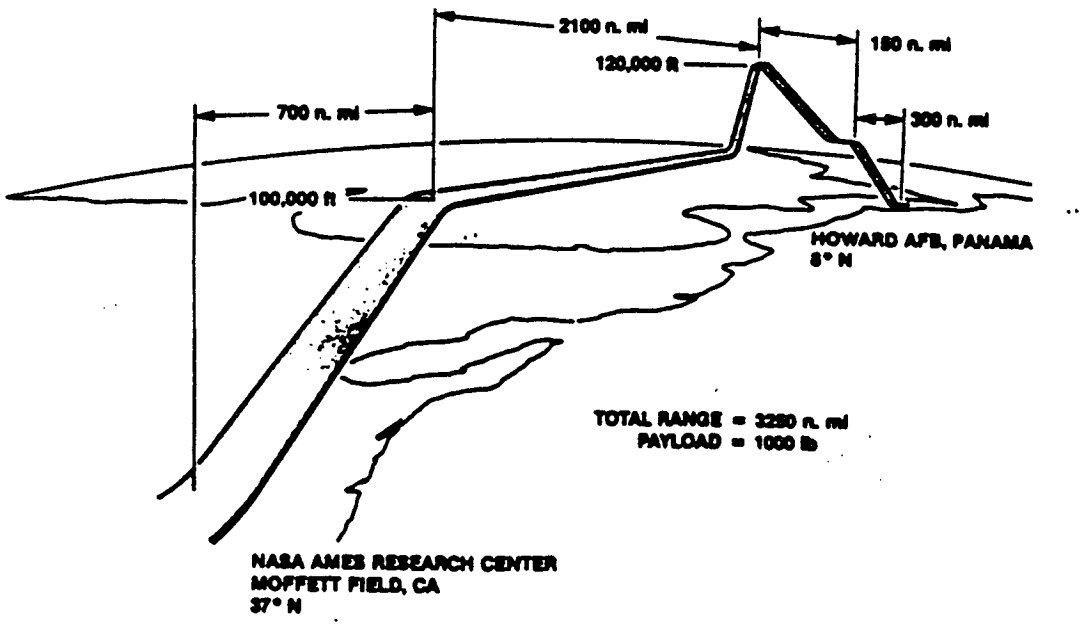

Figure 2.4.1 Mission four

about 100,000 ft over wide latitude ranges (5,000 n. mi.), to fly into the polar night, and to fly over the oceans far from land. The ability to jump up to 115,000 - 130,000 ft is required. The need to fly an integrated suite of particle and gas samplers and sensors, plus sophisticated radiometers, implies a payload capability of a thousand pounds.

3.0 DESIGN EVOLUTION

3.1 VEHICLE OPTIONS

Basic requirements for the aircraft are geographic coverage, sensing and sampling ability, payload capability, and effective duration. The vehicle needs to be able to cover the polar regions along with the midlatitudes. Sensing and sampling ability means the vehicle must be able to provide both remote and in-situ sampling. The payload the vehicle must be able to carry aloft will be between 1,000 to 4,000 lbs. The vehicle must also be able to stay aloft at an altitude of 100,000 ft for a worthwhile and effective length of time to accomplish the required information collection. At present, atmospheric studies are conducted through sounding rockets, research balloons, and airplanes.

Satellites are advantageous in that they provide a good global picture of the ozone situation. However, satellites are only able to provide remote sensing. Satellites can determine some of the stratosphere's chemistry, but cannot provide the important ability of collecting and examining samples at specific altitudes. Another disadvantage of satellites is their expense. Satellites cost millions of dollars to build, equip and launch. In addition, the reliability of successfully launching and positioning satellites is not excellent.

Sounding rockets have the advantage of being able to conduct both in-situ and remote sensing. For the payload size required, the rocket would be sufficiently large so that complex launching facilities would be needed. This means that geographic coverage provided by the sounding rocket would be limited since launching facilities for large rockets are limited. Sounding rockets are also "quick-look" vehicles. This

means the observation and sensing time at the required altitude would be short. Even though the unit cost of sounding rockets may be less than that of satellites, if the rocket is not reusable the cost of conducting a large number of experiments would probably escalate beyond reasonable limits.

At the present time, research balloons are the primary vehicle for stratospheric collection. They can conduct both in-situ and remote sampling. Research balloons are excellent in their ability to stay aloft for long durations at required altitudes, however, they must follow wind patterns and therefore cannot follow experimentally chosen paths. Another disadvantage is that even large balloon have payload limitations. Research balloons are also limited by the number of launch sites available worldwide. Another disadvantage of balloons is the difficulty involved in successfully recovering the payload and sometimes even payload loss.

The most current high-altitude airplanes still being used for atmospheric reconnaissance include NASA's ER-2 and DC-8 and the Boeing Condor. All three aircrafts are limited by their altitude ceiling. The DC-8 reaches approximately 45,000 ft and the ER-2 and Condor reach an altitude of 70,000 ft. Although current aircraft technology can not reach the required altitude, it was felt that an airplane could be designed to reach the required altitude and satisfy all other requirements better than any of the other vehicles mentioned.

3.2 CONFIGURATION REQUIREMENTS

The conceptual development for an aircraft to subsonically fly at altitudes of 100000+ ft began with the realization that, due to the extremely low densities at this altitude, the wing area and lift coefficient would have to be maximized and the weight minimized. Based on these three parameters with an airfoil selected to maximize C_l while minimizing C_d, and the mission specifications, the aircraft characteristics listed in Table 3.2.1 were used to evaluate possible aircraft configurations.

Table 3.2.1 Configuration requirements

- large wing area - minimum span, maximum aspect ratio
- maximize aerodynamic efficiency
- low wing tip bending or twisting
- minimize structural weight
- 360° sensor view
- ample ground clearance
- propulsion in line with center or gravity
- stability - on ground and in air
- internal storage volume (fuel, instruments)
- configuration simplicity

Five basic configurations were examined and their system level alternatives are listed in Table 3.2.2.

Table 3.2.2 System level alternatives

- Configuration
  - all-wing
  - monoplane
  - biplane
  - tandem wing
  - joined wing
- Manned versus unmanned
  - manned vehicle increases weight (600-800 lbs) and volume and limits endurance, but enhances aircraft flight test and landing capabilities.
- Launch
  - conventional runway (with landing gear or trolley)
  - carrier-aircraft drop
  - rocket launch or boost
  - balloon ascent

The first four of the following basic configurations were also examined with twin boom or twin fuselage modifications. The twin boom or twin fuselage designs reduced the required structural weight and bending moments of the aircraft by moving some of the weight outboard. This modification also made four-track landing gear possible, increasing the on ground stability of the aircraft. The downfall with these modifications was a marked decrease in aerodynamic efficiency due to increased drag caused by increased component interference and increased wetted area. In addition, much of the internal volume available in the mono-fuselage was lost when going to two fuselages of the same total weight. For these reasons, only single fuselage designs were considered for further analysis.

3.3 ALL-WING CONFIGURATION

The all-wing or flying wing design provides minimum frontal area and wetted area for reduced drag while yielding the greatest wing area. Interference drag is minimized by only having one component. The disadvantages with this design were primarily in the areas of weight, stability, ground clearance, and sweep. This design requires the wing to be highly swept for controllability which causes the loss of laminar flow over the wing reducing the aerodynamic efficiency. The high sweep of the wing and large span increase the required structural weight to prevent large tip deflections and this configuration's characteristic flutter. Flying wings can tolerate only a relatively narrow amount of longitudinal center of gravity travel, placing stringent requirements on the control

system and fuel management. This problem also greatly limits the payload feasibility of the aircraft. Ground clearance is a problem, requiring landing gear with struts up to 15 ft long or a trolley which greatly complicates landing.

3.4 MONOPLANE CONFIGURATION

The conventional monoplane has a large technical data base that helps to establish confidence in predicting structural and aerodynamic efficiencies and performance, but its advantages end there. The monoplane requires a very large span, approximately 400+ ft, large structural weights and landing gear similar to the flying wing. Very little can be done to improve tip deflections and wing twisting with this configuration. The required wing area and the resulting structural weight can never be equalized at an altitude of 100,000 ft for this configuration.

3.5 BIPLANE CONFIGURATION

The biplane provides the required wing area with half the span while still maintaining a high aspect ratio. Wing tip bending and twisting is reduced by the structural box formed by the two wings. Structural weight is reduced through inter-wing bracing and ground clearance is increased by mounting the propellers on the upper wing. Problems arise though in retaining the aerodynamic efficiency. Considerable losses result from wing to wing flow interference and mutual interference between the bracing and the wings. Additional structural weight is required to support the engines on the upper wing.

3.6 TANDEM WING CONFIGURATION

The tandem wing is similar to the biplane in maintaining the wing area while reducing span. This configuration sacrifices the additional structural integrity of the biplane in order to improve the aerodynamic efficiency by separating the wings. This aircraft now experiences ground clearance problems and propulsive unit location problems. The structural weight is still reduced for this aircraft as compared to the monoplane but is now larger than the biplane.

3.7 JOINED WING CONFIGURATION

As with the biplane and tandem wing configurations, the joined wing meets the required wing area with half the span while retaining a higher aspect ratio. Wing tip bending and twisting is reduced by joining the tips while aerodynamic efficiencies are maximized by spacing and separating the wings. Structural weight is reduced and ground clearance.Structural integrity in maintained through wing to wing joining, but aerodynamic problems are again similar to the tandem wing and biplane configurations. The joined wing configuration also experiences additional aerodynamic penalties though a reduction in the laminar flow over the rear wing due to its high sweep. Outrigger landing gear wheels and relatively long struts are required. The configuration is structurally more complex than a conventional design and performance analysis is also more difficult.

4.0 FINAL CONFIGURATION

The **SHARP** aircraft was derived to incorporate the advantages of the previous generic configuration while addressing their disadvantages. is shown in Figure 4.0.1. This aircraft was designed to cruise at 100,000 ft for over 5,000 n. mi. The aircraft is self propelled and launched from a runway, making it virtually independent of ground and air support. The finalized design allows for a wide range of flexibilities from supporting various instrumentation and payloads to rapid ease of conversion to a manned operational mode. The takeoff gross weight is 30,000 lbs and was sized to carry a 3,000 lb payload. A discussion of each aspect of the configuration is given below.

4.1 WINGS

The wing area is 4,000 ft^2 with a wing span of 250 ft. The aspect ratio of each wing is 31.25 and the taper ratio is 0.5. The mean chord is 8.44 ft with the inboard sections kept at a constant 10.0 ft chord to meet optimal airfoil characteristics at an altitude of 100,000 ft. An Eppler 1230 airfoil section was chosen to meet the demanding requirements of high-speed, low Reynolds number flight. A maximum coefficient of lift, C_l, is required from this airfoil at this altitude in response to the large drop in density. The outboard sections are tapered to 5 ft at the tip to create a more elliptical lift distribution and to reduce the required structural weight. At landing to reduce lift and ground roll distance, the drag is increased by deploying spoilers. For additional drag, the ailerons will be lowered to a -15 degree set point from which controllability is maintained. The wings are joined at the tips with a circular arc of radius 2.5 ft and chord of 5 ft yielding

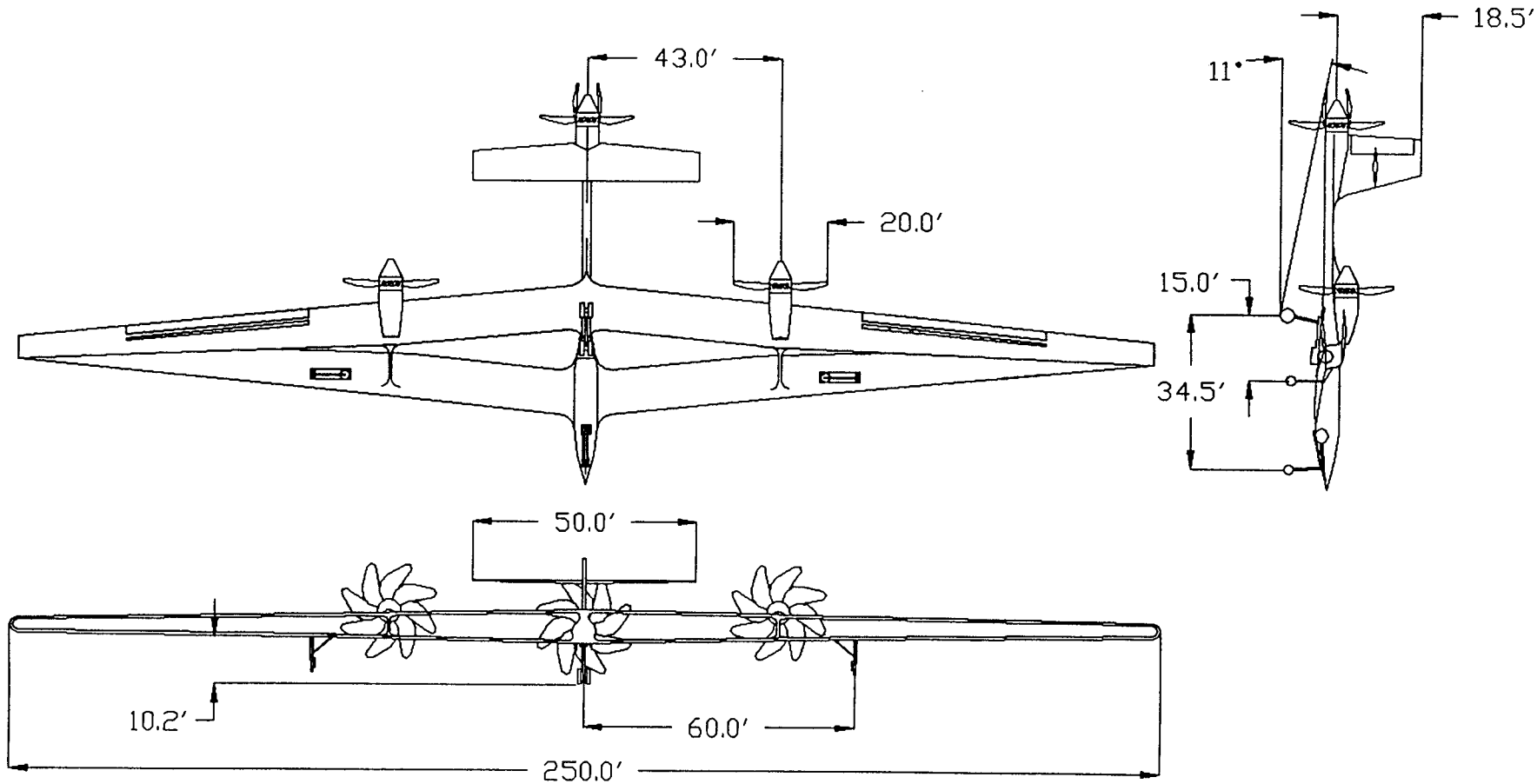

Figure 4.0.1 SHARP three view

a minimum wing spacing of 5 ft. This spacing was determined sufficient to avoid interference while allowing for structural integrity. The engines are mounted 43 ft outboard on the upper wings to provide additional ground clearance. Tapered inlet pods from the forward wing join the rear wing at the engine mounts providing additional structural integrity between the wings, higher speed flow into the engines as it passes over the forward wing and a passage for fuel from the storage tanks in the leading edge sections of the forward wing to the engines.

The construction materials in the wing will be 100% composite with the main spar being made of Spectra 1000. Spectra offers relatively high material stiffness (25,000,000 psi) and good tensile strength (435,000 psi). This causes Spectra to do quite well when subjected to bending loads.

4.2 EMPENNAGE

The horizontal tail will effectively act as an all moving control surface at center span of the vertical tail. This is required for both controllability at low densities and low wing loading landings. Incorporating an Eppler 1230 airfoil, the horizontal tail area is 375 ft^2 with a span of 50 ft. The center trailing edge is notched to allow for rudder movement. The vertical tail has an area of 225 ft^2 and a span of 25 ft utilizing a NACA 0009 airfoil.

As with the wing, the main substructure will be composed of Spectra 1000. This would reduce the component weights, hence making a lighter aircraft.

The folding propeller will be mounted aft of the tail section, driven by a shaft which extends from the rear of the fuselage pod to the gear box in the empennage.

4.3 PROPULSION

The propulsion system consists of three internal combustion, mono-propellent engines with three stages of turbocharging. The two primary engines are mounted in a pusher configuration on the upper wings. Fuel is routed through a tapered pod from the forward wing which also acts to accelerate the air flow into the inlet duct to improve the engine's efficiency. A 3-to-1 ratio gearbox was used to match the engines RPM and propeller speed to obtain high propeller efficiency throughout the flight regime. A single 20 ft diameter, eight blade, composite, propfan propeller was employed on each engine. The center auxiliary engine is located in the rear of the fuselage pod, forward of the main landing gear, with a drive shaft running back to the propeller mounted aft of the tail section. This propeller is mounted to the rear to allow easy conversion to a manned operational mode.

4.4 PAYLOAD

The payload will be located in trailing edge of the inboard sections of both wings and in the forward and center sections of the fuselage pods. These areas will provide excess volume, but this volume will be necessary to achieve a 360 degree antenna configuration. The excess volume also provides flexibility in packing the basic sensor suite, design flexibility in the avionics design, and is very adaptable to

alternative payloads. The infrared search and track is located in tandem sensors aligned longitudinally in a retractable pod under the center portion of the fuselage. This will allow 180 degree view forward and aft and during takeoff and climb may be retracted to reduce drag and prevent sensor damage. Panels will drop from the wings allowing easy access to all avionics and easy installation of alternative payloads. Antennas will be located longitudinally along the sides of the fuselage and along the trailing edge of the rear wing providing an unobstructed 360 degree view.

4.5 LANDING GEAR

The bicycle landing gear configuration was chosen for the aircraft. The main gears are located 45 ft from the nose (15 ft aft of the airplane's center of gravity) and support eighty percent of the total take-off weight. The nose gear supports the remaining twenty percent of the take-off weight and is located 5 ft from the nose. Both gears have a tire size of 12.50-16.

The landing gear is also coupled with outriggers that support the static wing loading and bending. They are located on the forward wing 65 ft from the tips which also enables the design to satisfy the 150 ft runway width. Tires were sized to carry engine and auxiliary equipment along the wing span, and as a result, 8.5-10 tires were used.

All gears and outriggers have strut lengths of 7 ft and all utilize an oleo-pneumatic shock absorber with a 1.2 ft stroke.

4.6 AVIONICS AND CONTROLS

The **SHARP** aircraft employs a stability augmentation system to insure level one flying qualities in all modes. Autopilots are used to control the aircraft for the unmanned missions, and to alleviate pilot workload during the manned missions.

4.7 RFP COMPARISON

SHARP can satisfy three of the four mission profiles. Since the absolute ceiling of the aircraft is 103,000 ft, it can not meet the Mission Four requirement of an excursion to 120,000 ft.

SHARP 's flexibility in converting between unmanned and manned flight modes makes it a viable vehicle for gathering upper atmospheric data.

SHARP's configuration allows it to meet and exceed all runway restrictions specified in the RFP.

SHARP meets the crosswind capability of 15kts, and can withstand moderate to severe turbulence.

SHARP is also equipped with three engines to provide both safety and flexibility during flight.

SHARP also meets the requirement for production by the year 2000. This is due to the extensive use of existing technology and materials on the configuration's airframe.

SHARP fails to meet is the hanger constraint of 110 ft x 70 ft, however the possibility exists that the aircraft could be made with detachable components.

5.0 PRELIMINARY SIZING AND WEIGHT ESTIMATION

From Reference #1, fuel weight percentage was determined by looking at the four different mission flight plans specified by the RFP. This method yielded a fuel weight ratio of 20%.

An initial weight estimation was needed to begin analysis of the proposed **SHARP** configuration. This was done using an initial weight estimation method in Reference #2 based on fuel and empty weight ratios. Assuming fuel weight is 20% of takeoff weight, an empty weight ratio similar to that of a composite cargo/bomber, and a 3,500 lb crew/payload, iterations were performed until the total takeoff weight converged to 1%. As a result, **SHARP** was initially calculated to be 32,000 lb.

Methods from Reference #2 were used to size **SHARP.** This method of sizing was based on properties of the atmosphere at cruise altitude. Assuming a cruise altitude of 100,000 ft, section lift coefficient of 1.08, Mach 0.6, and total gross weight of 29,000 lb, the sized values of **SHARP** located in Figure 4.0.1 were determined for a calculated wing loading of 6 psf.

A more specific method from Reference #2 was then used to estimate **SHARP**'s takeoff weight. This involves detailed dimensions of the aircraft configuration and approximated weights of the accessories such as hydraulics and instruments. Iterations were performed assuming **SHARP** undergoes maximum loads at takeoff. **SHARP**'s maximum gross takeoff weight was calculated to be approximately 30,000 lb.

6.0 MASS PROPERTIES

6.1 COMPONENT WEIGHT AND C.G. LOCATION

The methods used earlier in estimating takeoff weight were too general and did not necessarily comply with **SHARP**'s unconventional configuration. Thus, another weight estimation was made based on

Table 6.1.1 Component weight and c.g. breakdown

Component	Weight (lbs)	Fuselage Station (ft)	Water Line (ft)
wing	5000	30.8	10.3
horizontal tail	464	66.0	21.2
vertical tail	376	67.3	19.2
fuselage	1300	25.6	9.0
landing gear*	2000	5.1, 23.1, 37.8	5.2, 4.5, 5.8
STRUCTURES	9140		
engine^{g}	5700	35.9, 37.8	4.6, 13.5
propeller^{g}	1050	44.9, 83.3	14.1, 12.8
starting + control	110	19.2	8.3
fuel system	300	19.2	8.3
driving system + cooling	2840	21.8	8.3
PROPULSION	10000		
flight control	350		
instrument	10		
electrical	450		
flight avionic	700		
thermal system	300		
load + handling	50		
FIXED EQUIPMENT	1860	27.6	9.6
TOTAL EMPTY WEIGHT	21000		
fuel	6000	20.5	8.3
payload	3000	12.2	8.3
TOTAL	30000 lbs	28.3	9.8

* nose, outriggers, and main nose gear locations
^{g} forward and aft locations

acquired and calculated weights for different aircraft components such as engines and landing gear. Structural weight estimation was conducted based on an attainable composite weight to area ratio of

1.2 lb/ft^2. Wetted areas for the different components were then measured and multiplied by the 1.2 lb/ft^2 factor to give more accurate weight estimates. The aforementioned aircraft component weights are listed in Table 6.1.1. Figure 6.1.1 illustrates the component weight breakdown in percentages indicating that a majority of **SHARP**'s weight is propulsions, 33%, followed by structures with 31%.

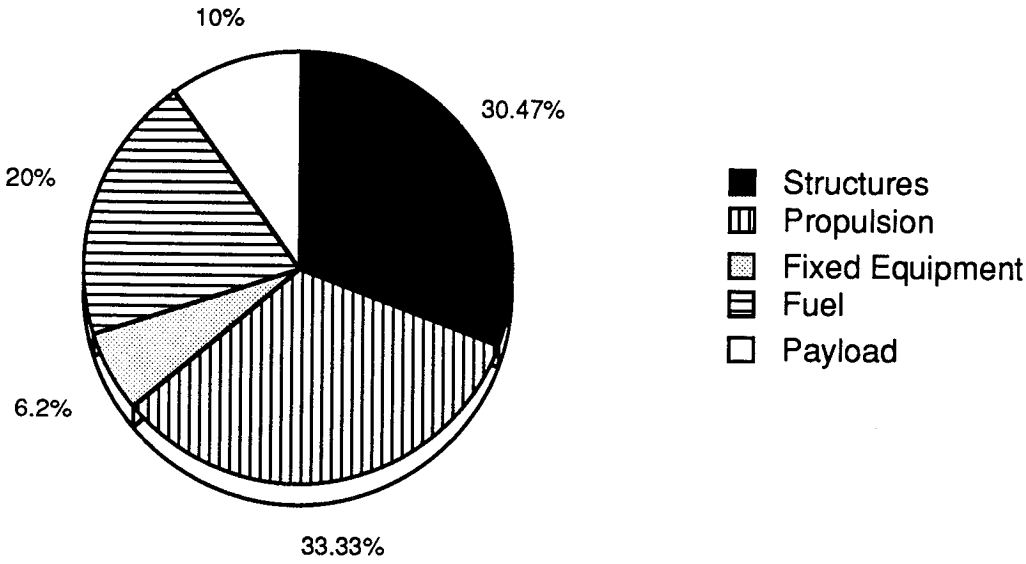

Figure 6.1.1 Weight breakdown at takeoff = 30,000 lbs

The location of the center of gravity was found by summing moments about the wing span and ground axis using the derived component weights. This location was approximated to be 28 ft from the nose and 10 ft from the ground.

7.0 PROPULSION SYSTEM

Propulsion system selection became one of the primary design drivers for the development of **SHARP.** It was important that the powerplant meet the RFP performance requirements of having long endurance and a cruise altitude of over 100,000 ft. Thus, a propulsive system that used relatively low amounts of fuel, had significant power at 100,000 ft, and a relatively low weight was selected.

7.1 ENGINE COMPARISONS AND SELECTION CRITERIA

Different propulsive systems were considered, including solar power, microwave beam riders, gas turbines, and reciprocating engines. Of these, reciprocating engines had the best balance between fuel consumption, power to weight ratio, size, and performance at 100,000 ft. Upon deciding on a reciprocating engine, the necessity to determine whether the engine should be a diesel or gasoline design was made. A diesel design is excellent for specific fuel consumption but inferior to a gasoline design when power outputs are considered. Hence, a gasoline cycle engine was chosen.

Next an engine configuration had to be selected. The four options investigated were radial, in-line, horizontally opposed, and v-design. The comparison between them can be seen in Figure 7.1.1, which compares weight, frontal area, and volume for each engine type assuming a 510 HP output at sea level. From the figure, the horizontally opposed engine offers the best combination of size and weight.

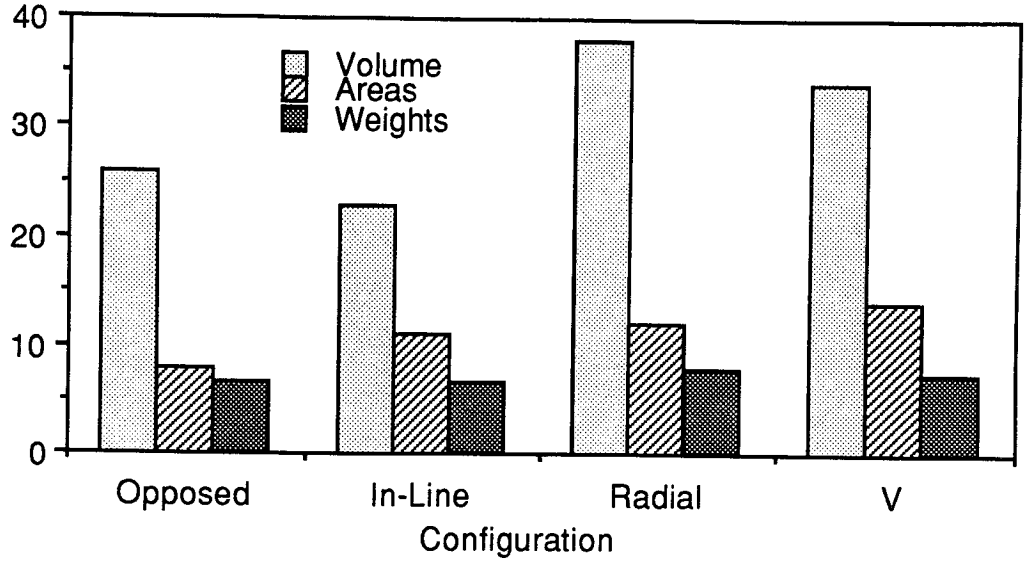

Figure 7.1.1 Engine configuration comparison

Based on the design constraints, a gasoline cycle, horizontally opposed engine became necessary. Fortunately, Teledyne Continental has plans for two such engines, the TSIOL-300 and the TSIOL-550. Both of the engines have three stages of turbocharging and are capable of operating at altitudes above 100,000 ft. The turbochargers are engaged at sea level, 40,000 ft, and 70,000 ft respectively, with maximum thrust maintained up to 100,000 ft . A study of estimated aircraft take-off weights and power requirements was made between the two engines (Figure 7.1.2). The TSIOL-550 engine is heavier, requires more fuel to cruise, and results in an overall heavier aircraft.

The required power for **SHARP** at 100,000 ft is 1,000 hp. If the TSIOL-300 engine is used, operation at full throttle for the entire climb and a significant portion of the cruise phase is needed. This would be stressful on the engine. Thus, the heavier yet more powerful TSIOL-550 was

chosen with three engines being the optimum number for **SHARP**'s mission requirements.

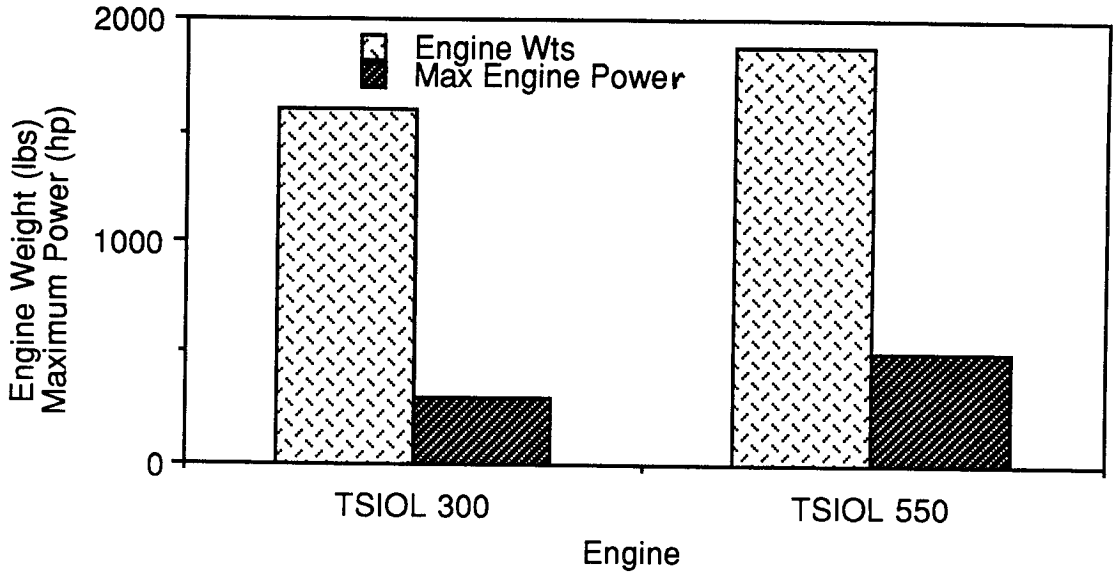

Figure 7.1.2 Teledyne engine comparison

7.2 DESCRIPTION OF ENGINE SELECTION

The TSIOL-550 was chosen for use on **SHARP** with a proposed variation of the existing TSIOL-550 Teledyne Continental engine. The engines are derivatives of the Voyager engine; hence, they have low specific fuel consumptions (0.45 lb/hr/hp, 100% power) and low weight (496 lbs, dry). The TSIOL-550, like its predecessor, is a liquid cooled, 550 cubic inch horizontally opposed six-cylinder engine with a frontal area of 9.88 ft^2, and a volume of 35.13 ft^3. Yet unlike its predecessor, it is turbocharged with three stages and a manifold pressure of 38.0 in. Hg at 500hp. The weight of the engine, turbochargers, and cooling system is

estimated at 1,884 lbs, resulting in a total weight for three engines of 5,652 lbs.

7.3 PROPELLER SELECTION

The selection of an optimal propeller design began with the determination of the critical operating parameters. The cruise flight regime was found to most severely effect the efficiency of the propeller. During cruise, the aircraft will be flying at Mach 0.6 at an altitude of 100,000 ft. The extremely low density at altitude requires the use of propellers with diameters close to 35 ft for a conventional design. The efficiency of a conventional propeller was shown to rapidly drop off at Mach numbers approaching 0.6. The solution to both the large diameter, which creates structural and clearance problems and the loss of efficiency at the higher speeds rests in the blade design. A modified prop-fan blade was developed for these flights conditions; thus, reducing the required diameter to 20 ft while maintaining an efficiency of 0.86. Additional analysis has shown the design to provide sufficient efficiencies during all other flight regimes.

The propeller to airframe and engine integration for the two main engines is shown in Figure 7.3.1. The propeller consists of eight highly swept blades, each attached by means of a variable pitch mechanism to a central hub with a diameter of 5 ft. A blade sweep of 38 degrees was selected to optimize efficiency, while reducing noise levels produced by the propeller by 8 dB. The net efficiency increases resulting from the blade sweep has been predicted to be 3% . Each propeller blade will consist of a NACA Series 6T airfoil from the root to 37%

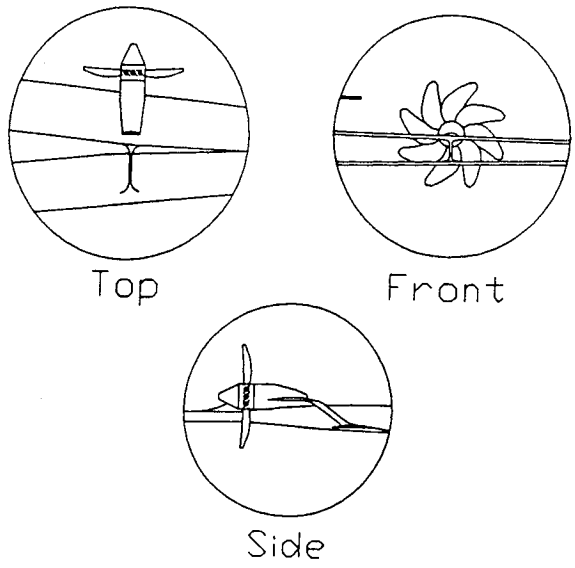

Figure 7.3.1 Main engines integration

span, an ARA-D airfoil from 45% span to the tip, and a tapered region from 37% to 45% span. Based on the 4 ft chord at 70% span of each blade, the advanced ARA-D airfoil increases the overall efficiency by 13% over the conventional NACA series 16 airfoils.

The variable pitch mechanism is required to achieve maximum efficiencies during all flight regimes and to maintain a satisfactory fan-surge margin which can be critical on low pressure ratio fans. The variable pitch mechanism allows for appropriate positioning of the blades in the tail auxiliary engine for collapse. The blades in the auxiliary propeller are hinged such that they fold simultaneously around the central hub as shown in Figure 7.3.2. The folding of the propeller is required for additional clearance, particularly during takeoff rotation. For simplicity and reduction of weight, the blades are spring loaded and open purely due to centripetal force.

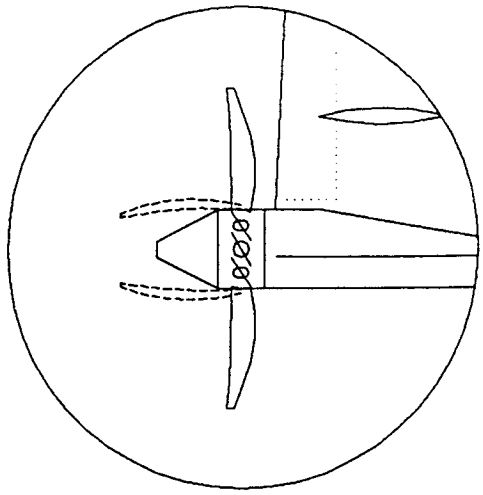

Figure 7.3.2 Auxiliary propeller

The blade construction will consist of a single, full span, boron-aluminum composite spar and a boron-epoxy composite shell. A foam fill will be used in all remaining open areas within the shell. A nickel sheath will be placed on the leading edge of each blade for additional impact and corrosion resistance. Approximately 50% of the spar fibers will be micro-coated with nickel for lighting conductivity. The total weight of each propeller assembly is 330 lbs with an additional 14 lbs required to fold the auxiliary propeller.

The pusher configuration implements special problems in blade fatigue. Each time a blade passes through the wake of the wing or empennage it experiences a different loading than the freestream condition. But because the material of the blade is largely composite, cyclic loading is not expected to be a major concern. Also, because the blades are modular, they can be regularly tested ultrasonically for delamination or fatigue.

7.4 ENGINE COOLING

Normally, engine cooling is not a design driver in the design of an aircraft. Most engines are simply cooled with air flow over the engine's radiators. However, the density of air at 100,000 ft is 1.4%the density of air at sea level. The extremely low density results in making radiators so large that the cooling drag produced is three times the entire aircraft drag. Therefore, to cool the the engines and avoid the drag penalty, an alternative method of engine cooling was designed.

Instead of conventional radiators, forced convection and radiation is to be used to cool the engines. The engine's coolant and oil are each pumped separately over the wings in a thin layer an eighth of an inch thick, Figure 7.4.1. The thin layer is to be covered with anodized aluminum, because of its low cost, low weight, and high emissitivity, 0.87. The hot fluids are to heat the aluminum, which is cooled by convection and radiation to the atmosphere.

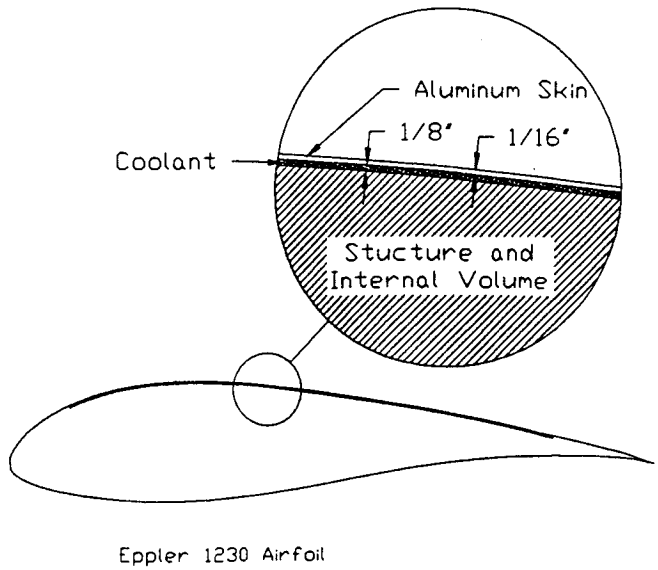

Figure 7.4.1 Airfoil cooling detail

At cruise the turbochargers produce 403 Btu/s, while the engine produces 292 Btu/s. The engine coolant carries off 211 Btu/s and the oil 81 Btu/s. The coolant is also to be used on the turbochargers; therefore, the coolant needs to cool a total of 614 Btu/s.

The airflow over the top wing is to be cooled by convection, 0.1942 Btu/s ft^2. In addition, radiation to the atmosphere will result in a heat transfer of 0.0922 Btu/s ft^2. Combining the two results in a heat transfer of 0.2864 Btu/s ft^2. The wing area, Figure 7.4.2, therefore needed to cool the coolant is 2,145 ft^2 and the engine oil is 283 ft^2. The areas are readily available on **SHARP**. The weight penalty for this cooling method is the additional coolant to be carried,1,500 lbs, and the aluminum 1,400 lbs.

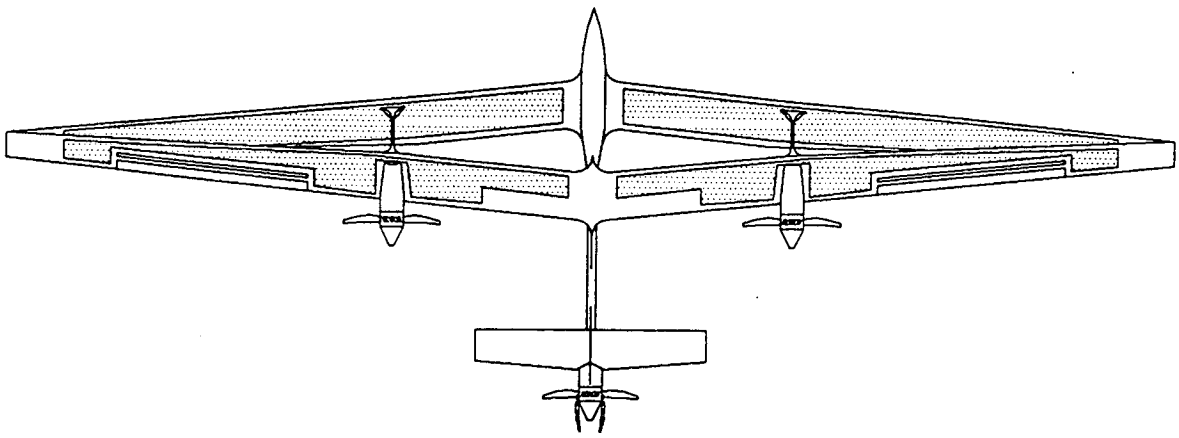

Figure 7.4.2 Required cooling area

8.0 AERODYNAMICS

8.1 AIRFOIL SELECTION

For the worst case of 100,00 ft, a Reynolds number of 600,000 was used to obtain an airfoil that gave the best performance at this altitude. For the investigation, three airfoils were analyzed (1) Wortmann FX67K-170/17; (2) Eppler 1233; and (3) Eppler 1230. The factors used in choosing the Eppler 1230 were the comparison of endurance parameters, $C_l^{3/2}/C_d$ and $C_{l\ max}/C_{d\ operational}$, figure of merit graph, and L/D (Table 8.1.1) .

Table 8.1.1 Airfoil endurance parameters

AIRFOIL	$C_l^{3.2}/C_d$	$C_{l\ max}/C_d$ @ C_l operational	L/D
FX67K-170/17	29.40	37.74	24.46
Eppler 1233	25.47	25.24	40.31
Eppler 1230	53.67	61.76	53.67

Keeping $C_l^{3/2}/C_d$ as large as possible maximized the rate of climb and the endurance for the aircraft. The airfoil selected would be used on the wing and the horizontal tail and $C_l^{3/2}/C_d$ does not give quantitative numbers for that type of airfoil use. However, the largest value of $C_{l\ max}/C_{d\ operational}$ would be beneficial for quantitative analysis and so it was used. Of the three airfoils, the Eppler 1230 had an average value 50% higher for both parameters.

A figure of merit graph looks at the drag polar plots of the airfoils (Figure 8.1.1). The objective of the graph is to obtain the maximum value of C_l for a minimum amount of C_d. If two airfoils have the same amount

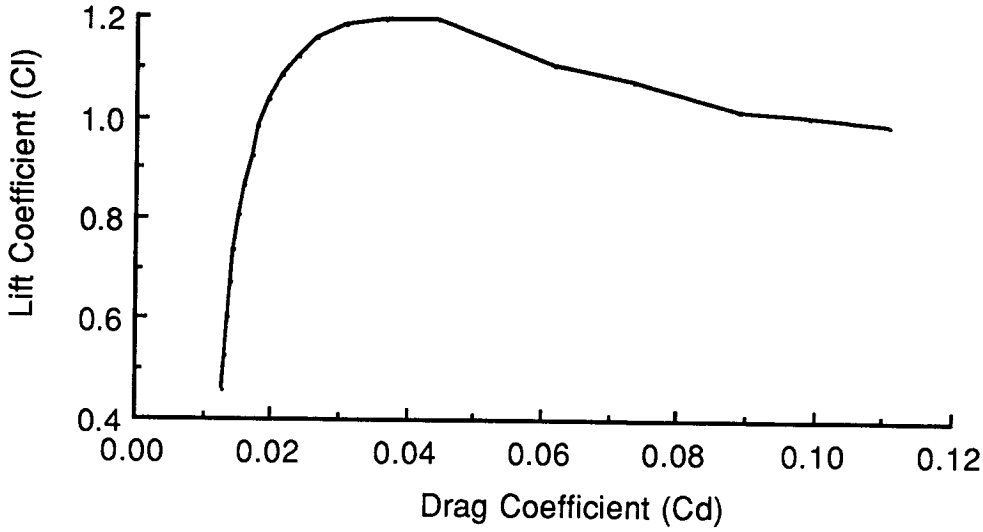

Figure 8.1.1 Eppler 1230 drag polar

of C_d, the one with the larger C_l would be chosen. A higher C_l would represent a lower surface area which in turn would result in a lower wetted surface area drag. Even though the FX67K-170/17 had a 10% higher value of C_l, the Eppler 1230's 22% savings for C_d was preferable.

Lastly, the airfoil with the largest amount of L/D was important in selecting an airfoil. A large value of L/D would give enough lift for the given amount of drag present and the Eppler 1230 provided that with a L/D of 53.67.

The Eppler 1230 was chosen at an alpha of 4 degrees, for it produced the highest value of C_l for a minimum drag (C_l = 1.0805, C_d = 0.02131, Figure 8.1.2). A maximum thickness of 18% occurring at 26% chord will provide for useful volume area for fuel, engines, and landing gear

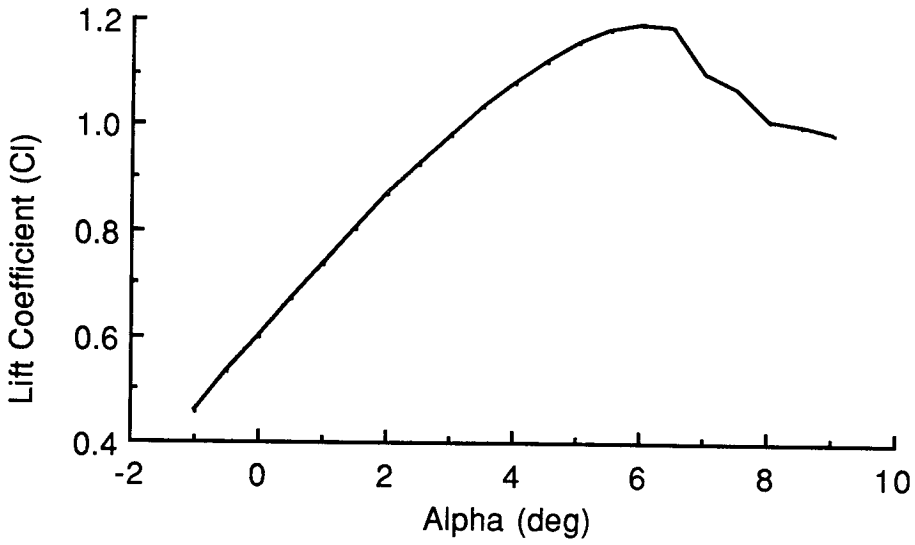

Figure 8.1.2 Eppler 1230 lift curve slope

storage. At the root, the chord would be 10 ft while the tip would only be 5 ft.

Tapering the wings for increased aerodynamic efficiency lowers the chord Reynolds number. Tests were performed to insure that airfoil efficiency stayed at satisfactory levels.

8.2 REFERENCE GEOMETRY

As shown in Figure 4.0.1, the reference geometries for **SHARP** are noted in Table 8.2.1.

Table 8.2.1 Reference geometries

S_{ref}	wing planform area	4,200 ft^2
c_{mg}	mean geometric chord	8.40 ft
b	wing span	250 ft

These numbers were used for the determination of all other parameters used in this analysis.

8.3 LIFT DETERMINATION

Using the methods for determining lift for a biplane configuration found in Reference #3, the geometry for an aerodynanmically equivalent mono-wing was calculated. With the dimensions of this known, it was then possible to use the optimization methods in Reference #4 to maximize the lift-producing efficiency of the two-winged craft.

One simplifying factor in the analysis of lift production is the absence of high-lift devices in the wings. Because of the extremely low wing loading, these devices are not required for takeoff or landing and would actually reduce the cleanliness of the composite airframe while increasing its weight and cost.

Unless unwarranted assumptions of airframe cleanliness were made, the wings, configured in their current fashion, are able to support the weight of the aircraft (minus its burned fuel) at the insertion altitude of 100,000 ft.

8.4 DRAG DETERMINATION

The aerodynamic drag on the airframe was calculated using methods presented in Reference #2. Because this reference accounts only for turbulent flow, it represents a worst-case approximation for the calculation of drag coefficient. In actuality, laminar flow would exist over

much of the flying surfaces (up to 20% from the leading edge), even at low Reynolds numbers. The calculated numbers were therefore reduced approximately 18% over the wings and empennage sections. The resultant contributions to aerodynamic drag are shown comparatively in Figure 8.4.1.

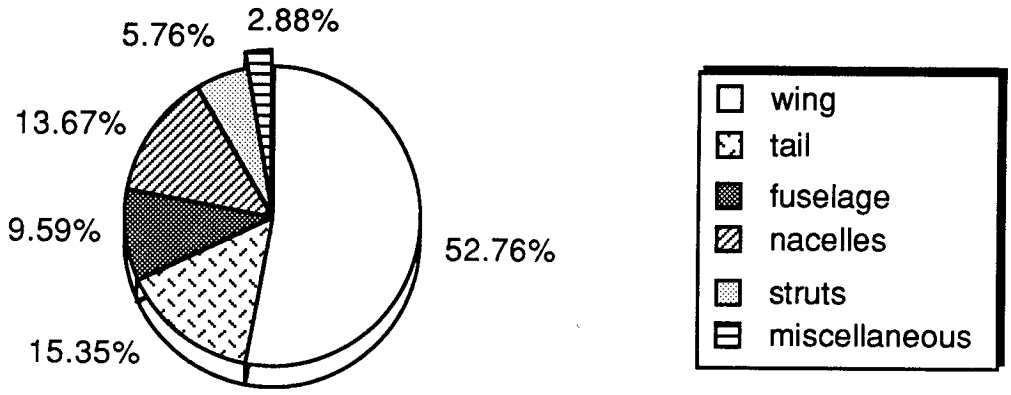

Figure 8.4.1 Drag breakdown, 1023 lbs

The total configuration drag coefficient is 0.0417 which translates to a drag estimate of 1,023 lbs at on-design conditions.

Because forced convection and radiation are used to cool the engines, and because these heat exchangers are located on the upper surface of the wing, no direct flow interference is involved in reducing the temperature of the engine coolant or intercoolers. The boundary layer on the upper wing surface, however, is certainly energized by the addition of heat energy to the flow. Its actual effect on the aerodynamic behavior of this craft, however, is beyond the scope of this analysis.

9.0 MATERIALS and STRUCTURES

9.1 MATERIAL SELECTION AND BREAKDOWN

A comparison of various materials was conducted to determine which material(s) would give the optimum performance for **SHARP**. As with all aircraft structural materials, weight was the primary selection criteria, with lighter materials being favored over heavier for obvious reasons.

The seven materials considered for **SHARP**'s structural configuration were stainless steel, aircraft aluminum, titanium, graphite/epoxy, boron/epoxy, aramid/epoxy (Kevlar 49), and Spectra 1000. These materials were compared according to stiffness (elastic modulus), tensile strength, and strength to weight ratio. The results of this comparison can be seen in Figures 9.1.1-3. The advanced materials, Kevlar and Spectra 1000 were chosen.

Kevlar and Spectra 1000 also have other advantages. Both have good resistance to corrosion, and cracks in the material tend not to propagate as quickly as in metals. Kevlar is also extremely impact resistant, which is an added protection against possible bird strikes. Preliminary reports also indicate that Kevlar and Spectra 1000 are resistant to fatigue, and as widespread usage increases, other benefits will become evident. The only drawback to these two materials is cost. Presently, these materials are extremely expensive with Kevlar over $10 per pound. Hence, the cost of the aircraft increases dramatically with the use of Kevlar and Spectra 1000. However, as more and more structures begin to incorporate these materials, prices should drop, making them even more attractive.

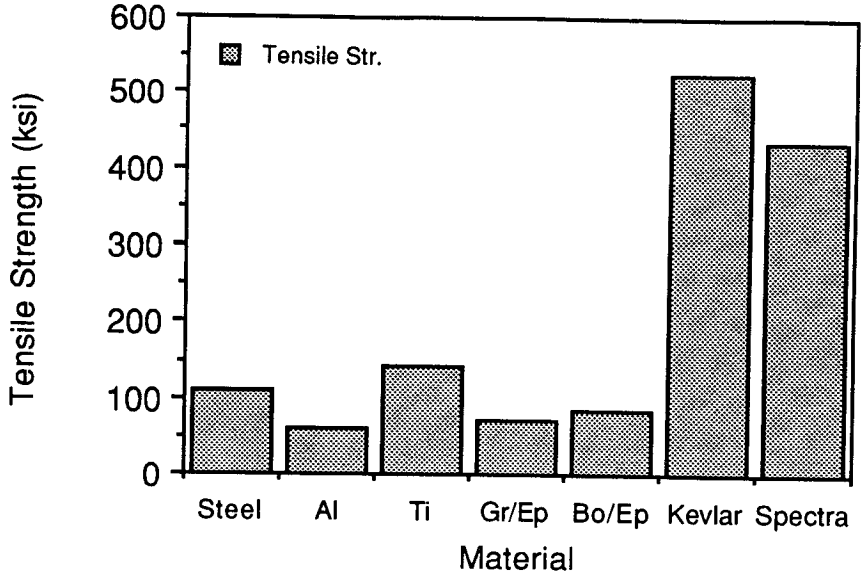

Figure 9.1.1 Material tensile strength comparison

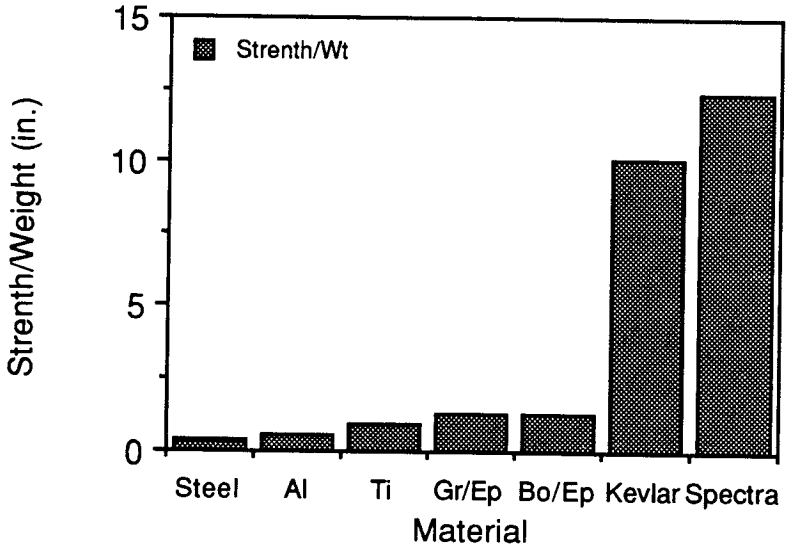

Figure 9.1.2 Material strength to weight ratio comparison

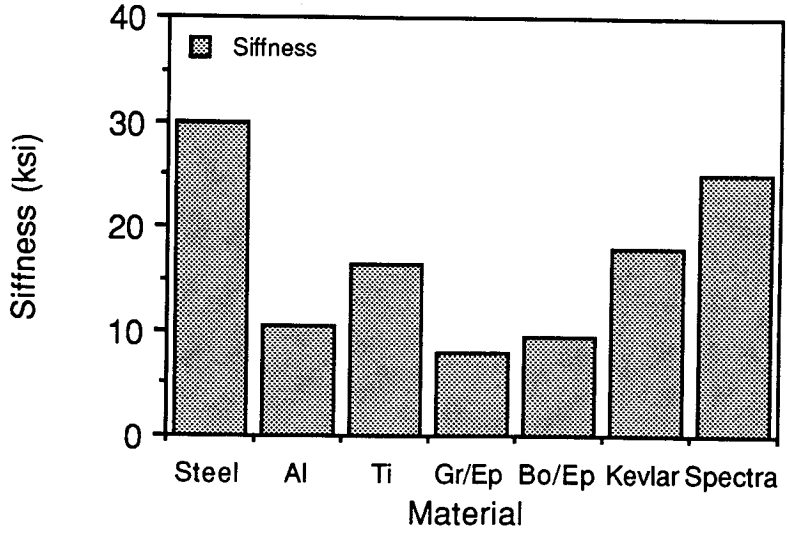

Figure 9.1.3 Material stiffness comparison

9.2 STRUCTURAL ANALYSIS

The joined wing design of **SHARP** offers a host of structural advantages. Being a biplane, the aerodynamic loads on each wing are halved, and the joined wing offers additional rigidity to the wing. A preliminary analysis indicates that the outer edge of the joined wing will deflect less than 12 ft due to a gust load of 2.25 (Figure 9.2.1). This analysis assumes a single-spar wing made of Spectra 1000, with a spar cross-section of approximately 17 square inches, moments of inertia Iy = Iz = 1192 in^4, a shear web of 0.25 in., and a height of 20 in. The joined wing also keeps the wing from twisting during flight, as evidenced by a calculated 1.2 degree twist angle at the wing tips. Analysis also yields that the main spar will weigh approximately 898 lbs.

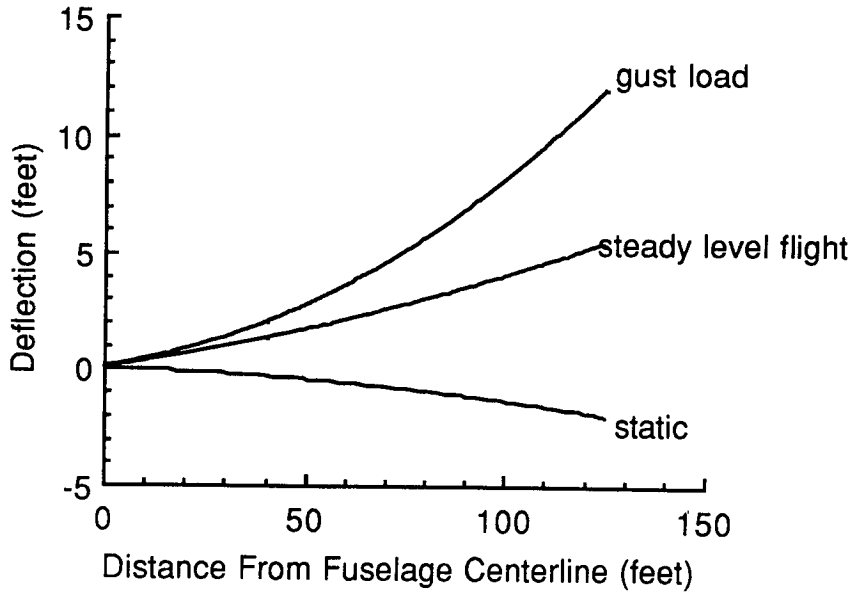

Figure 9.2.1 Wing deflections

Due to the tremendous length of the wing, the torque box will have to support a bending moment of 690,000 lbs-ft (Figure 9.2.2), and a shear force of 11,300 lbs (Figure 9.2.3). To withstand these forces a rather bulky structure will be developed, however, the exact specifications of this structure are yet to be determined.

Preliminary analysis also indicates that the aft fuselage section will have to withstand a 12,000 lbs-ft downward bending moment due to the weight of the engine, propeller, drive shaft, and the horizontal and vertical tail. The aft fuselage will also have to withstand the torque of the engine drive shaft. The effects of that torque are to be determined in future analysis.

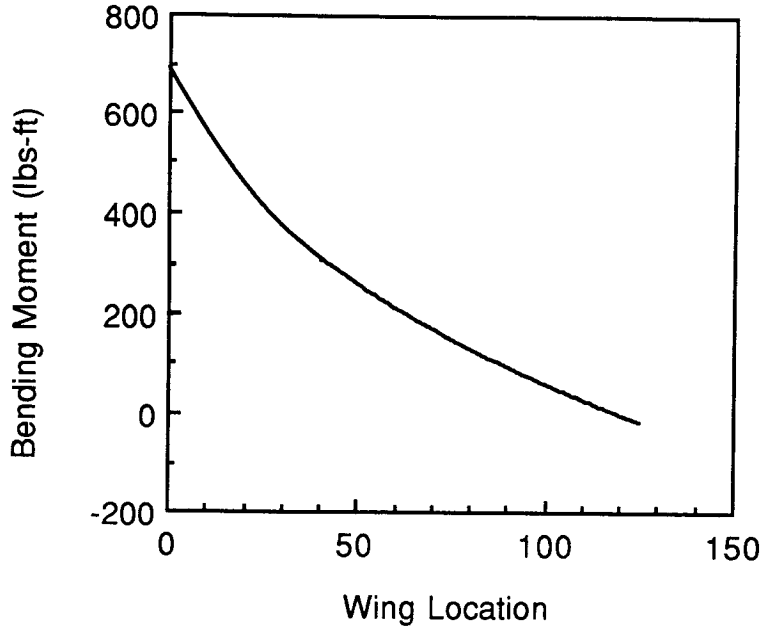

Figure 9.2.2 Bending moments along main spar

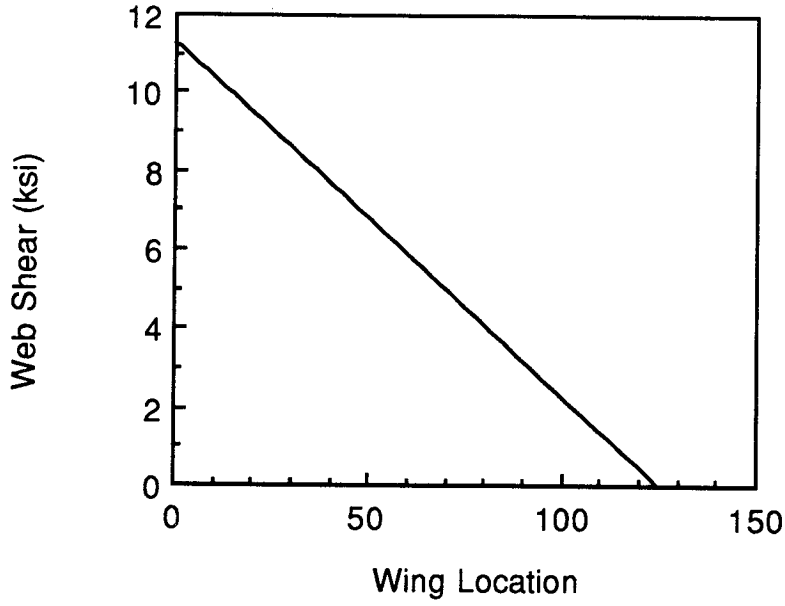

Figure 9.2.3 Web shears along main spar

9.3 V-n DIAGRAM

Flight load factors, n, are the ratios of aerodynamic force components to the weight of the aircraft acting normal to the longitudinal axis of the aircraft. Positive flight load factors are those acting upwards opposing the weight of the aircraft. Constructing a velocity-load factor diagram will aid in determining the structural integrity of **SHARP.** In this way, the aircraft can be designed to withstand such aerodynamic forces. The V-n diagram depicted in Figure 9.3.1 combines the maneuver and gust envelope to determine the flight envelope for **SHARP** at 50,000 ft. It is at this altitude that **SHARP** will encounter maximum loads. A V-n diagram for the cruise condition of 100,000 ft was determined, Figure 9.3.2. This was combined with the flight envelope at 50,000 ft to yield a more general envelope, Figure 9.3.3. As depicted the maneuver envelope is encompassed by the flight envelope. Thus, a majority of the flight envelope is dictated by gust loads allowing for little if any maneuverability. **SHARP** may be maneuverable up to load factors of 2.75 and -1.1. But because the aircraft is not designed for high performance, maneuverability is not of great concern. As a result, **SHARP** was designed to primarily suppress gust loads that may occur during the flight mission.

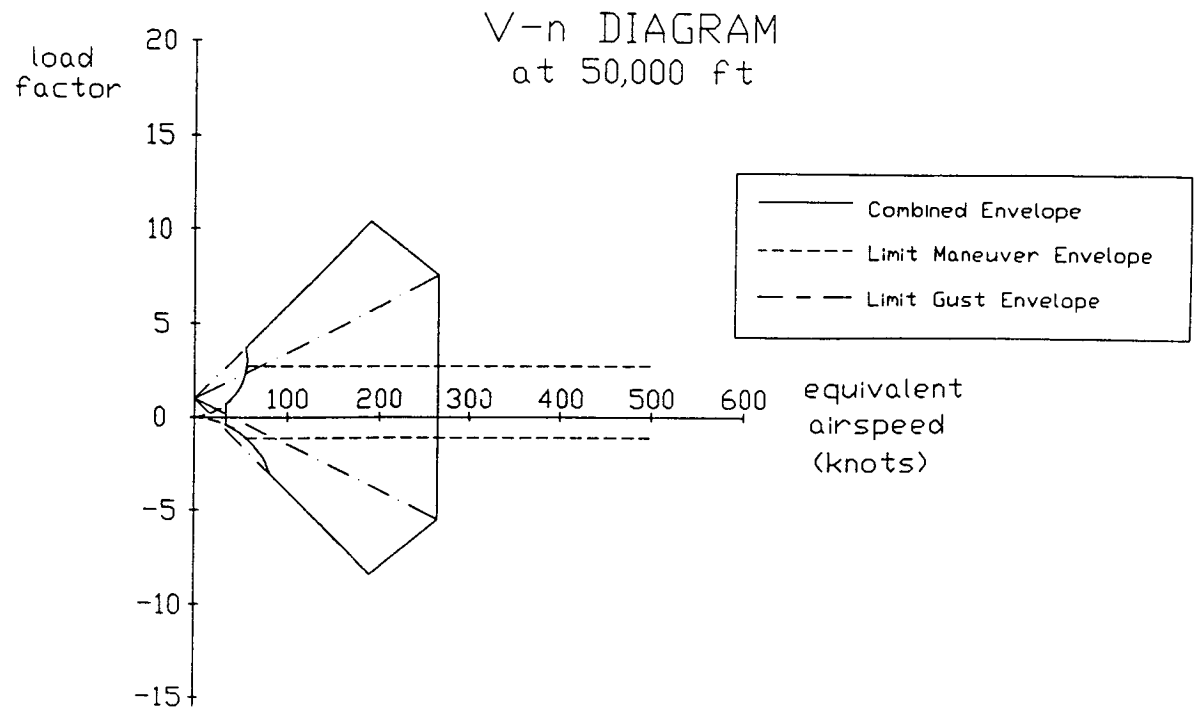

Figure 9.3.1 V-n diagram at 50,000 ft

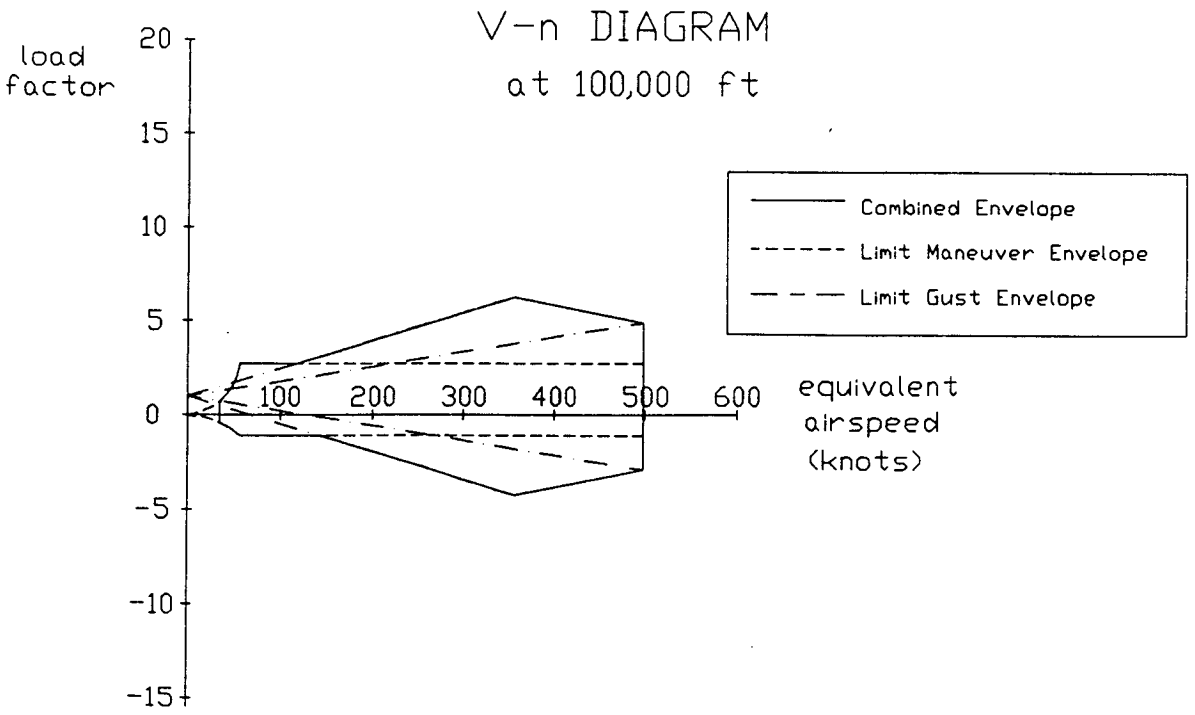

Figure 9.3.2 V-n diagram at 100,000 ft

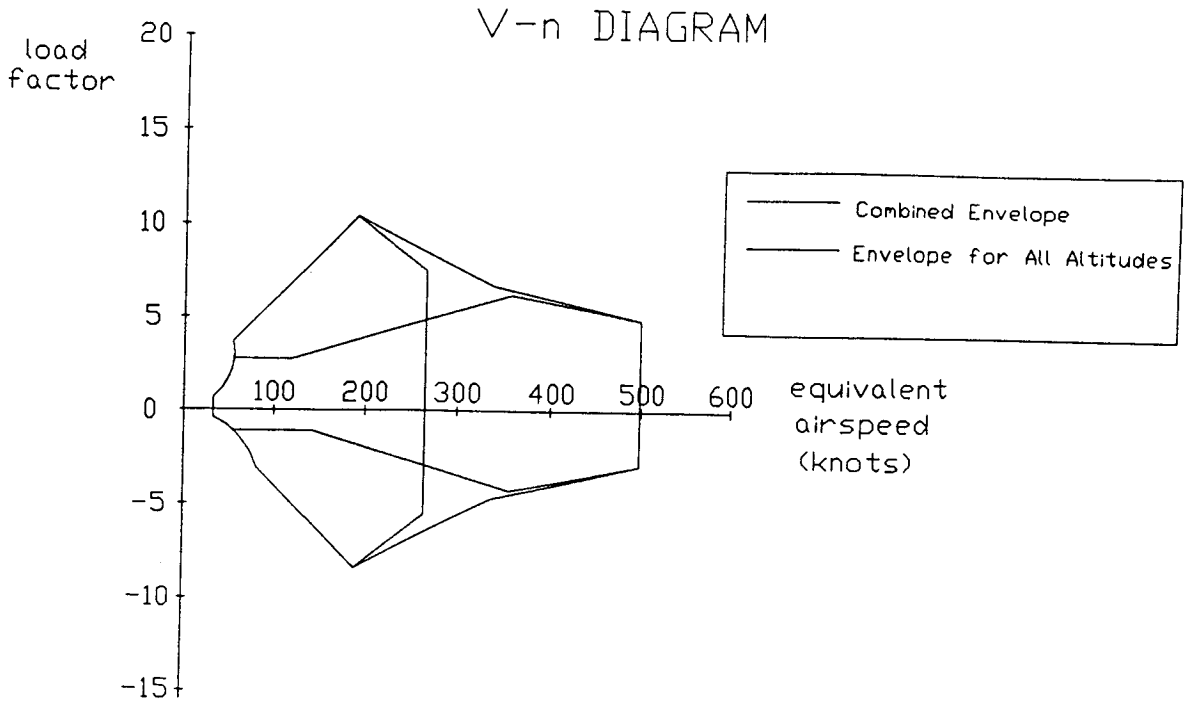

Figure 9.3.3 Combined V-n diagram

10.0 STABILITY AND CONTROL

10.1 STATIC STABILITY DERIVATIVES

A spreadsheet program developed from Reference #5 was used to calculate **SHARP**'s static stability derivatives. These calculations were based on a flight condition of 100,000 ft altitude, flying at Mach 0.6, and a cruise weight of 27000 lb assuming 3000 lb of fuel burned for climb. Table 10.1.1 summarizes the static stability derivatives for the aforementioned flight condition.

Table 10.1.1 Static stability derivatives

Longitudinal Derivatives	Lateral Derivatives
$C_{Lu} = 0.780$	$C_{y\beta} = -0.187$
$C_{mu} = 0$	$C_{l\beta} = 0.154$
$C_{Du} = 0$	$C_{n\beta} = 0.0020$
$C_{L\alpha} = 7.58$	$C_{yp} = -0.0086$
$C_{m\alpha} = -2.47$	$C_{lp} = -0.703$
$C_{D\alpha} = 0.258$	$C_{np} = -0.213$
$C_{Lq} = 9.61$	$C_{yr} = 0.0060$
$C_{mq} = -15.3$	$C_{lr} = 0.467$
$C_{Dq} = 0$	$C_{nr} = -0.0213$

Note that the longitudinal damping derivatives, $C_{m\alpha}$, C_{mq}, and $C_{L\alpha}$, have the required signs for longitudinal static stability. Therefore, although the horizontal tail appears comparatively small to the large wing span, its size is adequate to serve as an effective longitudinal stabilizer.

Lateral damping derivatives are shown to satisfy static stability requirements, except the dihedral effect, $C_{l\beta}$. Because the vertical tail

has such a large area, $C_{l\beta}$ is positive. As a result, the dihedral effect is large in which the side force on the vertical tail due to sideslip increases producing a yaw and rolling moment. Although this may seem undesirable, the rolling moment produced by the vertical tail tends to bring the aircraft back to a wings-level attitude. If the resulting oscillatory motion due to the static instability of $C_{l\beta}$ diverges, then a stability augmentation system will be utilized to actively stabilize the aircraft.

10.2 DYNAMIC STABILITY

SHARP as defined by Reference #6 is classified a class II, category B airplane. Though the aircraft does not require "in-flight refueling," the other phases (i.e. cruise, climb, descent) do apply.

The dynamic responses, longitudinally and lateral, of the aircraft are presented in Table 10.2.1.

Table 10.2.1 Aircraft response at 100,000 ft

Mode	Frequency	Damping Ratio	Time Constant
Phugoid	0.0919	0.0416	
Short Period	0.8730	0.2590	
Spiral			145.98
Roll			0.0825
Dutch Roll	—	—	

Longitudinally, AFDA time simulations reveal that the aircraft's dynamic responses converge when given step inputs. The phugoid damping response of 0.0416 classifies the aircraft as level 1. However,

the short period damping response makes **SHARP** a level 2. This is acceptable because the magnitude of the short period is quite small (1.25 degrees) and will damp out within 20 seconds. A problem did arise with CG excursion and its effects on the dynamic response of the aircraft: as fuel is used, the fuel tanks located in the lower forward wing will lighten, causing the value of $C_{m\alpha}$ to become less negative. This problem will hopefully be resolved by pumping extra coolant into the forward wing toward the end of the mission.

Laterally, the spiral and roll modes display a level 1 response. For **SHARP**, dutch roll natural frequency and damping ratio were not present, possibly due to software errors or misuse or the fact that the configuration is so unique.

10.3 STABILITY AUGMENTATION SYSTEMS

In order to insure stability and level 1 flying qualities, the **SHARP** is equipped with stability augmentation systems. The Dutch roll mode is one mode of concern for the **SHARP**, because of the reasons mentioned in the section above. The root locus diagram for the Dutch roll mode of the uncompensated aircraft is shown in Figure 10.3.1. As can be seen from the figure there is inadequate damping. In order to insure level one flying qualities in the Dutch roll mode, a Dutch roll damping stability augmentation system will be employed. Figure 10.3.2 is a block diagram of a Dutch roll damper.

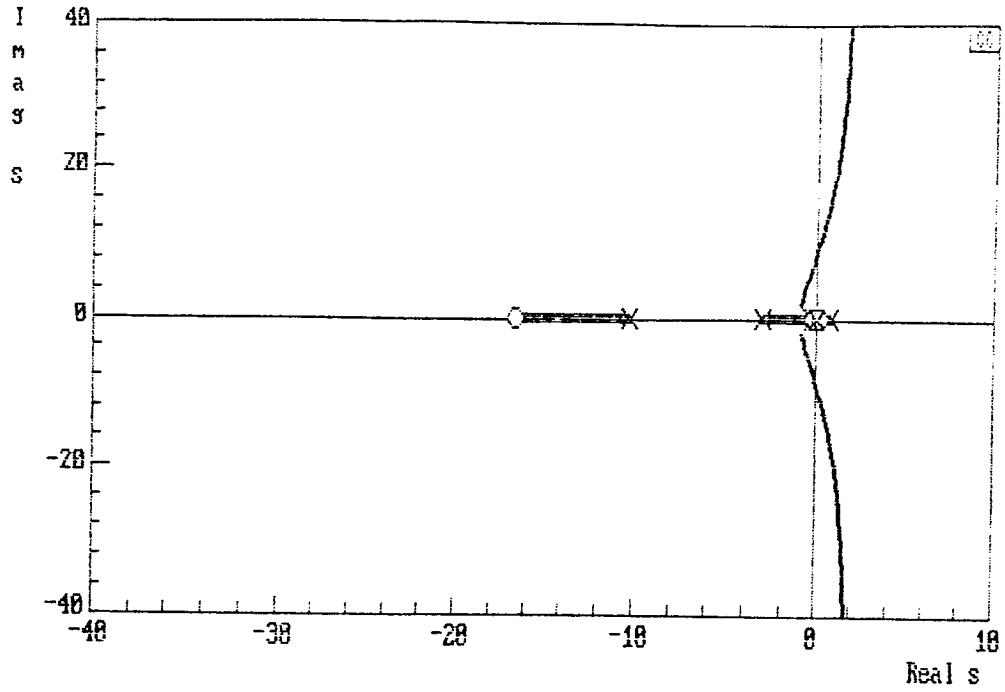

Figure 10.3.1 Root locus diagram for uncompensated aircraft

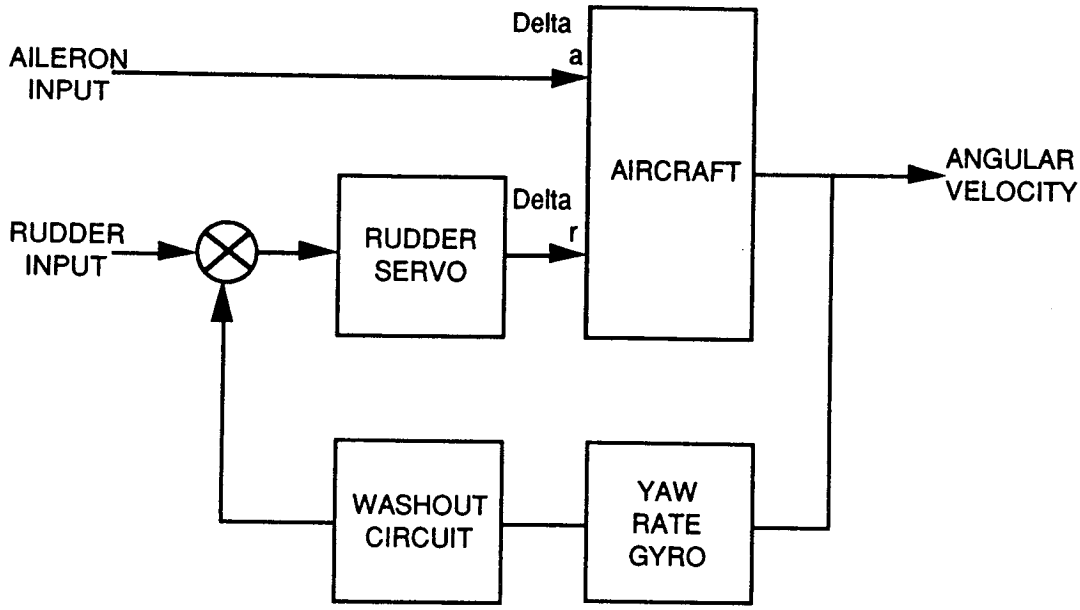

Figure 10.3.2 Block diagram of Dutch roll damper.

The washout circuit in the block diagram produces an output only during the transient period. According to Reference #6, this is due to the fact that if the yaw rate signal did not go to zero in the steady state, then for a positive yaw rate the output of the yaw rate gyro would produce a positive rudder deflection. This would result in an uncoordinated maneuver and require a larger rudder input for coordination. The transfer function for the washout circuit used is s/(s+1). The rudder servo is -20/(s+10), while the yaw rate gyro gain is 21.5. The root locus diagram for the compensated aircraft system is seen in Figure 10.3.3.

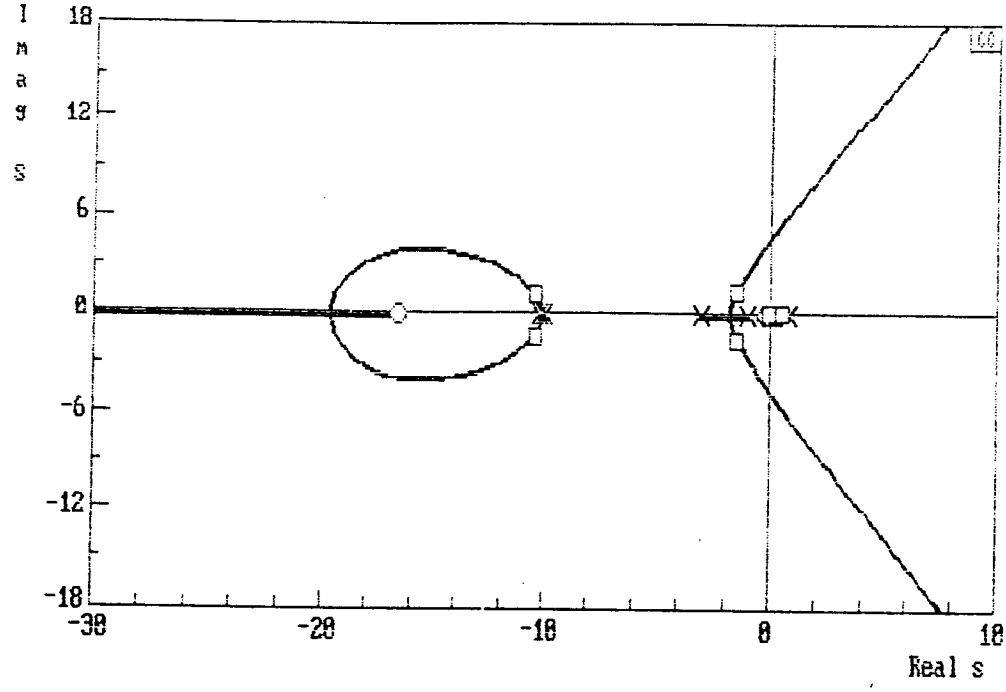

Figure 10.3.3 Root locus diagram for compensated aircraft

This root locus yielded a damping ratio of 0.706 and a natural frequency of 2, which qualifies as level 1 flying qualities.

The remainder of the modes will also be made level 1 with the use of stability augmentation systems.

11.0 AUTOPILOTS AND AUTONOMOUS CONTROL

The **SHARP** aircraft will be equipped with autopilot systems to control the aircraft while it is unmanned. The autopilots will also relieve pilot workload for those missions where the **SHARP** is manned. The autopilots will work with all the stability augmentation systems to control all modes of the aircraft.

11.1 PITCH DISPLACEMENT AUTOPILOT

An example of one of the autopilots on the **SHARP** is the pitch displacement autopilot. The pitch displacement autopilot is designed to hold the aircraft in straight and level flight by controlling the aircraft's pitch angle. The autopilot is shown in a block diagram in Figure 11.1.1.

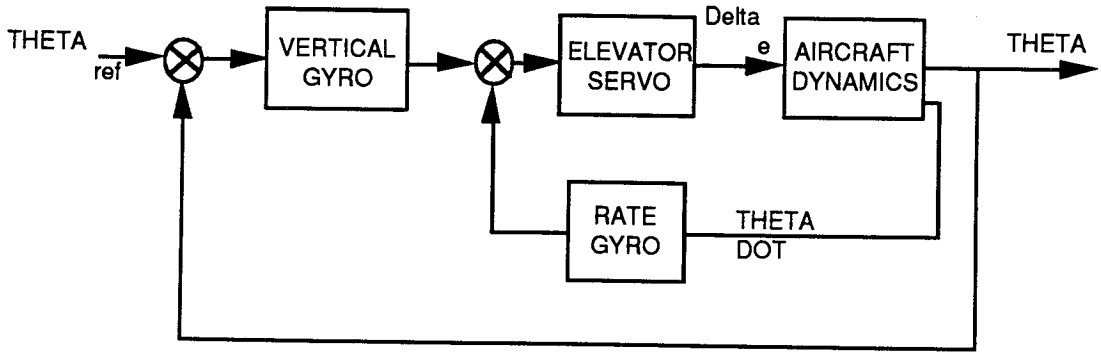

Figure 11.1.1 Pitch displacement autopilot block diagram

The vertical gyro gain is 2.0. The elevator servo used is -(s+1)/(s+20). The negative is used to produce a positive output for a positive input, due to the fact the aircraft transfer function contains a negative. The rate gyro gain used is 10.15. The autopilot employs rate feedback for added

damping. The damping of this system is 0.700. The damping was determined from the root locus plot of the system, which is shown in Figure 11.1.2.

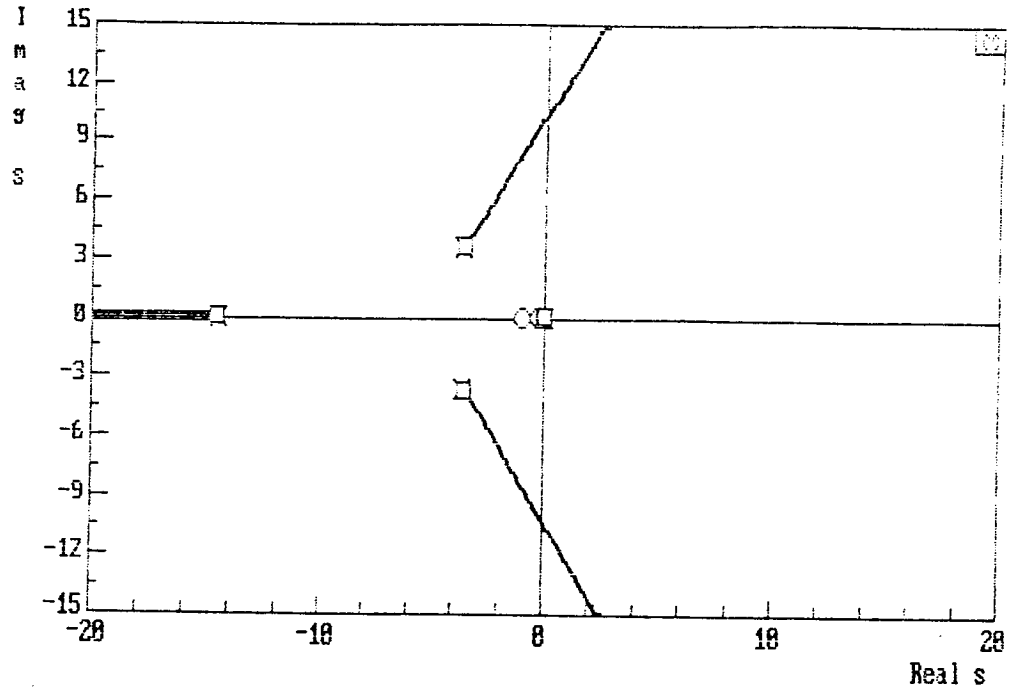

Figure 11.1.2 Root locus diagram of pitch displacement autopilot

The time response of the autopilot system is shown in Figure 11.1.3. The time response is for a unit step elevator input. The plot shows that there is no overshoot and that it takes 120 seconds to achieve the steady state value.

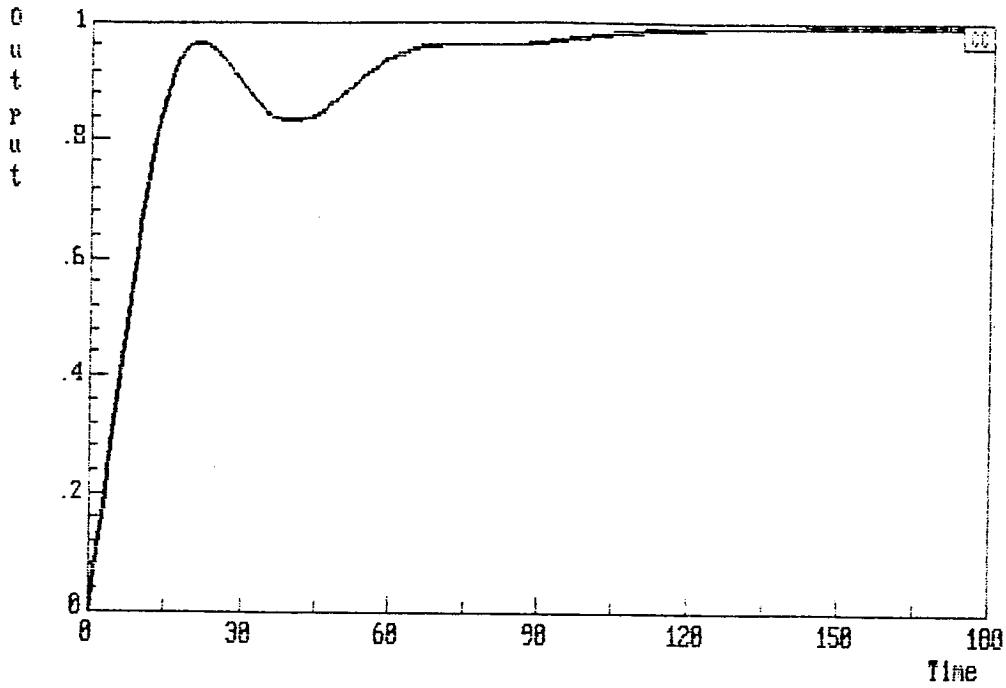

Figure 11.1.3 Time response of the pitch displacement autopilot

12.0 PERFORMANCE

12.1 FLIGHT ENVELOPE

The flight envelpe for the **SHARP** aircraft under standard day conditions can be seen in Figure 12.1.1. This envelope maps the combinations of altitude and velocity that the aircraft is capable of operating within. The minimum flight velcity for a given altitude is based on the stall speed of the wing airfoil. The maximum flight velocities are given by the maximum thrust output from the propulsion system. The maximum velocity trend shown in Figure 12.1.1 assumes a continuous rate of turbocharging. The level of turbocharging has been selected to maximize power output while maintaining a safe engine manifold pressure. At the design cruise altitude of 100,000 ft a flight envelope of 30 knots is obtained. The maximum operating altitude for the aircraft under RFP specifications is 105,000 ft.

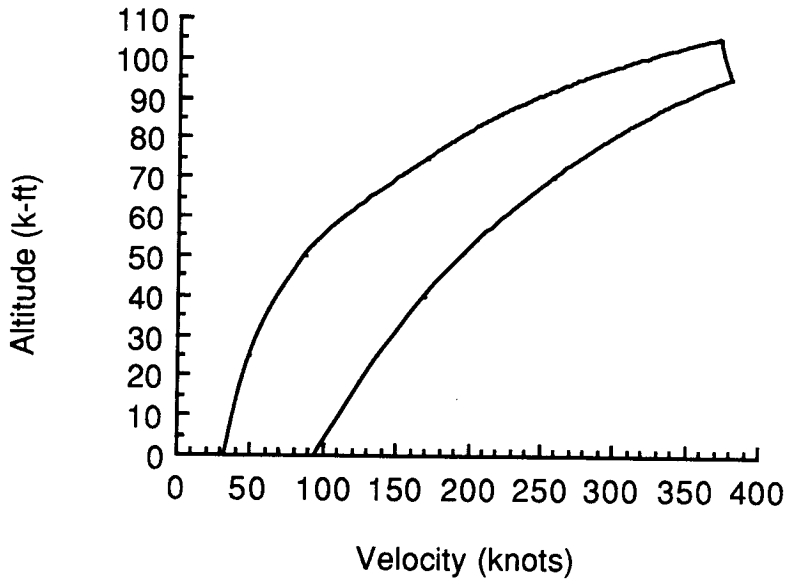

FIGURE 12.1.1 Flight envelope

12.2 TAKEOFF PERFORMANCE ANALYSIS

From calculations, a takeoff distance of 973 ft is required. This assumes that the three TSIOL-550 engines would produce 500 HP or equivalently 8,250 lbs of thrust total at takeoff. Breaking down the runway into distances for ground roll, transition, and climb, lengths of 631 ft, 318 ft, and 24 ft are needed. For the transition to climb phase, the aircraft would be at 949 ft down the runway. It is at this point that the aircraft makes the transition at 43 ft off the ground with a climb angle of 15 degrees. This is too steep of a climb for the **SHARP**. A resolution of the problem was found by using only two engines for takeoff. With two engines, less fuel is needed for takeoff at runway length expense of 1,259 ft. Though this would make the runway 23% longer, it does not matter because the extra runway is needed if the balanced field length (BFL) requirement is to be satisfied. For three engines, BFL was 1,604 ft and only 1,708 ft for two. The use of two engines decreases the climb to 9 degrees. This also eliminates the roll-out problem that would be associated if the auxiliary engine was operating at takeoff. According to landing gear calculations, **SHARP** could handle a 11 degree angle of pitch. Though only two engines will be used at takeoff, the FAR obstacle requirement of 50 ft is still satisfied. Thus, the runway length is 1,259 ft, with 863 ft allotted for ground roll, 197 ft for transition and 200 ft for climb.

12.3 LANDING PERFORMANCE ANALYSIS

The analysis of landing is the reverse of takeoff. The equations used in determining the takeoff distance is again used in calculating landing distance. For the approach distance, 838 ft is needed for a

velocity of 110 ft/s at an angle of 3.23 degrees. The aircraft will flare at a velocity of 105 ft/s for a distance of 96.3 ft. When the aircraft touches down at 101 ft/s, an allotment of 301 ft is given for free roll assuming 3 seconds before brakes are applied. Upon the application of the brakes, **SHARP** will travel 886 ft before stopping. Therefore, the total landing distance is 2,122 ft. But to satisfy the FAR requirement an additional length of 1,415 ft is added. This increases the required runway length to 3,537 ft.

12.4 ENGINE CLIMB PERFORMANCE:

Based on the available horsepower from the three engines, the weight of the aircraft, and various atmospheric qualities, preliminary analysis indicates that the **SHARP** will have a rate of climb as shown in Figure 12.4.1. Based on this, the time for the aircraft to climb 100,000 feet

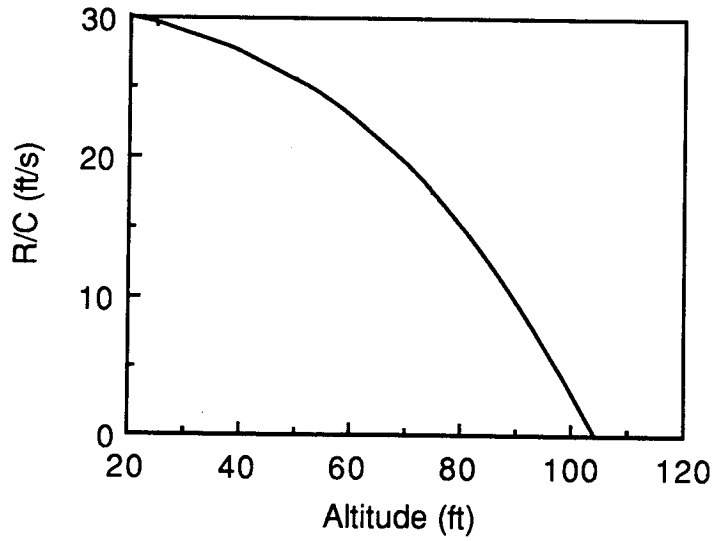

Figure 12.4.1 Rate of climb

was calculated, and determined to be approximately 4.1 hours (Figure 12.4.2). Knowing the SFC of the engines, the power requirements, and

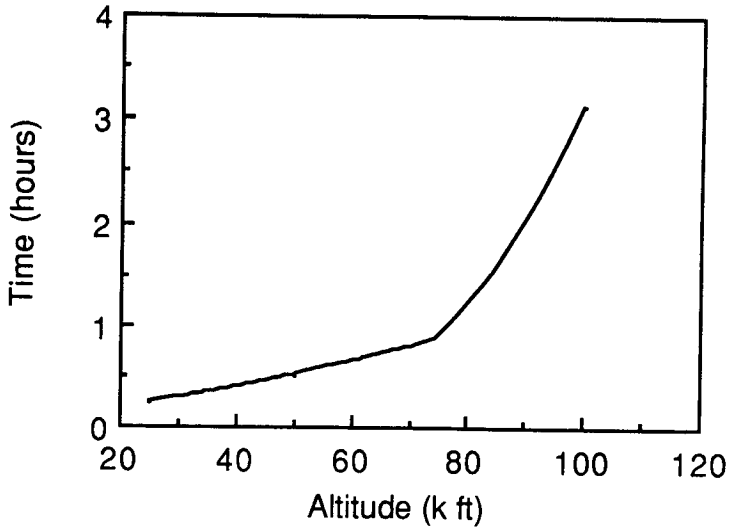

Figure 12.4.2 Time to climb

the time to climb, yielded the required fuel for the climb portion of the mission (Figure 12.4.3), and led to the total amount of fuel required for the entire mission, which was approximately 6000 lbs.

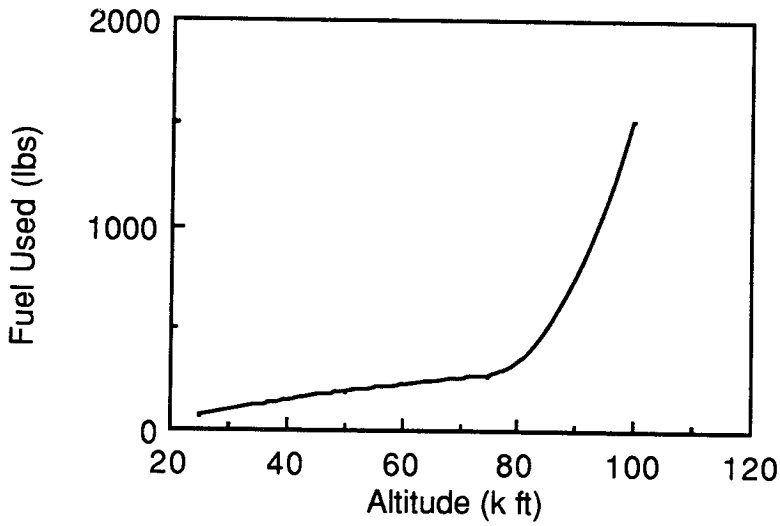

Figure 12.4.3 Fuel to climb

13.0 SYSTEMS DESCRIPTION

13.1 MODULAR PAYLOAD AND INSTRUMENT PACKAGE

In order to provide easy access and serviceability to the avionics and payload components, the design of the **SHARP** configuration stresses the use of modular components, a paramount example of which is the detatchable nose section of the fuselage. This nose section contains the majority of the avionics hardware as well as the payload and instruments which will be used to sample atmospheric data.

Figure 13.1.1 shows the general design of the detachable nose section. It is 28 ft long and slides into a structural sleeve formed by the forward section of the fuselage and is held by several latch mechanisms. Electrical connections between the avionics packages and servomechanisms consist of plug units at the rear of the pod and the forward section of the fuselage.

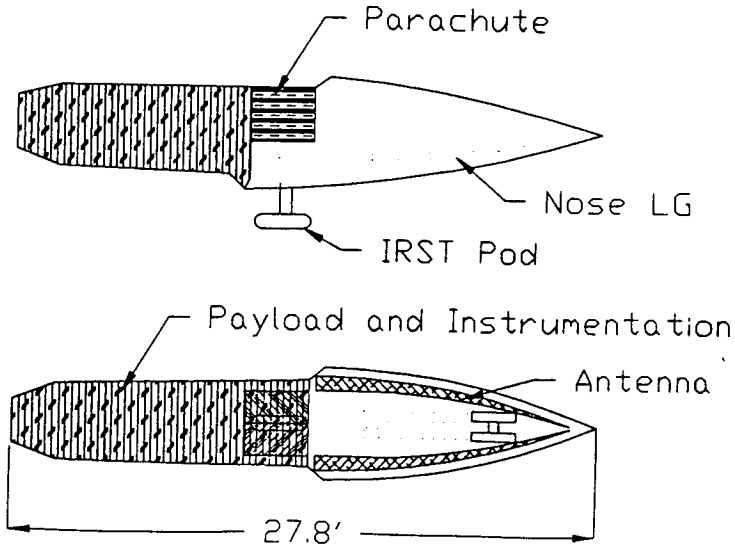

Figure 13.1.1 Detachable nose detail

In case of a structural failure or unrecoverable flight condition, the detatchable nose section can be ejected away from the rest of the craft and a parachutes deployed to slow its descent. The ejection process is activated by the detonation of a small mortar charge at the rear of the pod. At detonation of these charges, a guillotine mechanism will sever the electrical connections for both the flight control system as well as the atmospheric sampling devices.

Two parachutes will be used to slow the descent of the pod. The first is a small drogue parachute used to orient the pod in a horizontal manner and begin an initial decelleration. This parachute will be used above 50,000 ft altitude so as not to be greatly affected by gusting atmospheric winds. Below 50,000 ft the larger main parachute will be deployed. Its surface area of 20,000 ft^2 will slow the descent rate to 10 ft/sec at sea level. The stowed volume of both parachutes is 27 cubic ft.

The use of a modular pod also allows the consideration of manning the craft. Figure 13.1.2 shows a six-foot-eight pilot seated in a modified pod. This pod contains suitable volume for the storage of the required life control systems and preliminary studies show that the shift in the CG location does not create a stability problem. But if the flight of **SHARP** is to be manned, human factors and life support systems must be considered.

To ensure normal breathing conditions when flying at altitudes of 60,000 ft or greater, not only must the air breathed be enriched with oxygen, but the pressure surrounding the pilot must be raised. This is achieved when the pilot wears a pressure suit. Absolute pressure in the

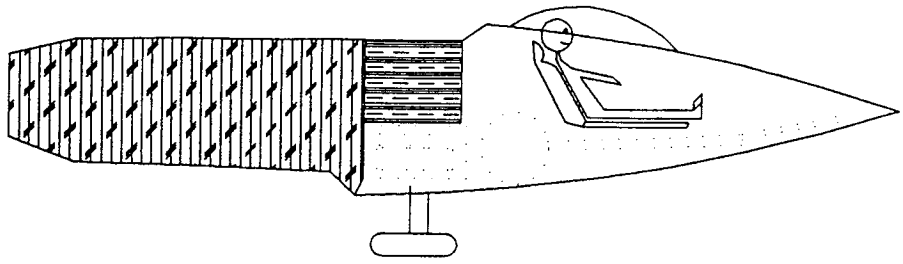

Figure 13.1.2 Pilot modified pod

suit must correspond to air at a maximum of 33,000 ft. For extended flight times, more pressure is required.

Keeping in mind that the pilot will be in a pressure suit, the cockpit must be large enough so that the full pressure suit will fit and that there is adequate access for life support technicians to integrate the pilot into the cockpit. Oxygen and suit cooling air sources must be provided. The controls, displays, instruments and circuit breakers must be accessible and within visual range when the pilot is completely outfitted in the pressure suit and the pilot strapped into the cockpit.

13.2 ELECTRICAL SYSTEM

Electrical power for the on-board flight systems is generated using alternators on the 3 engines and as such is triply redundant. Power output is generated in alternating current (AC) and can be converted to direct

current (DC) based on the power requirements of the on-board instrumentation and payload. All connections are modular in nature to support ease of exchange or service.

13.3 FUEL SYSTEM

Figure 13.3.1 shows the location of the fuel tanks in the wing. The tank volume is sized to hold 6,000 lbs of aviation fuel and the internal structure of the tanks contain anti-slosh baffles to prevent dynamic oscillations. Fuel filling locations are located on the top surfaces of the front wings. Fuel lines for the outboard engines are routed through the inter-wing struts. The auxilliary engine receives fuel through lines located along the sides of the fuselage. Because of the fuel lines' proximity to the mission termination mortar charge, control valves will be employed to stop the flow of fuel during the separation phase of the mission abort.

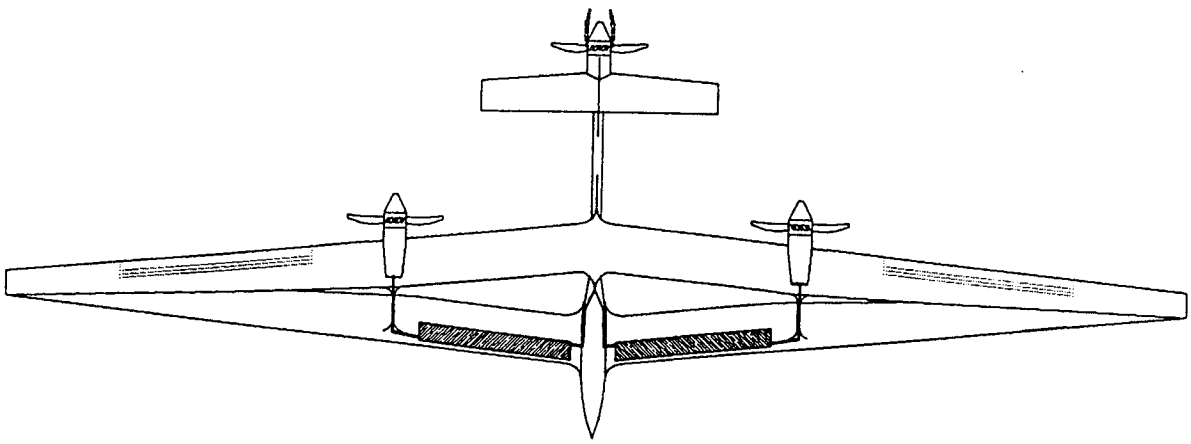

Figure 13.3.1 Fuel tank location

13.4 LANDING GEAR

Through observation, a bicycle landing gear configuration was chosen. This would be coupled with wing gear located on the forward wing of the aircraft to serve as training wheels. Thus, if the wings should tip to either side, the wing gear could prevent the propeller blades on the aft wing from touching the ground. Internal weight locations were varied to determine an optimum location for the wing gear, Figure 13.4.1. The spanwise location of the supportive wing gear was at the c.g. of either side of the wing, 65 ft from the wing tips. Although the gap between the

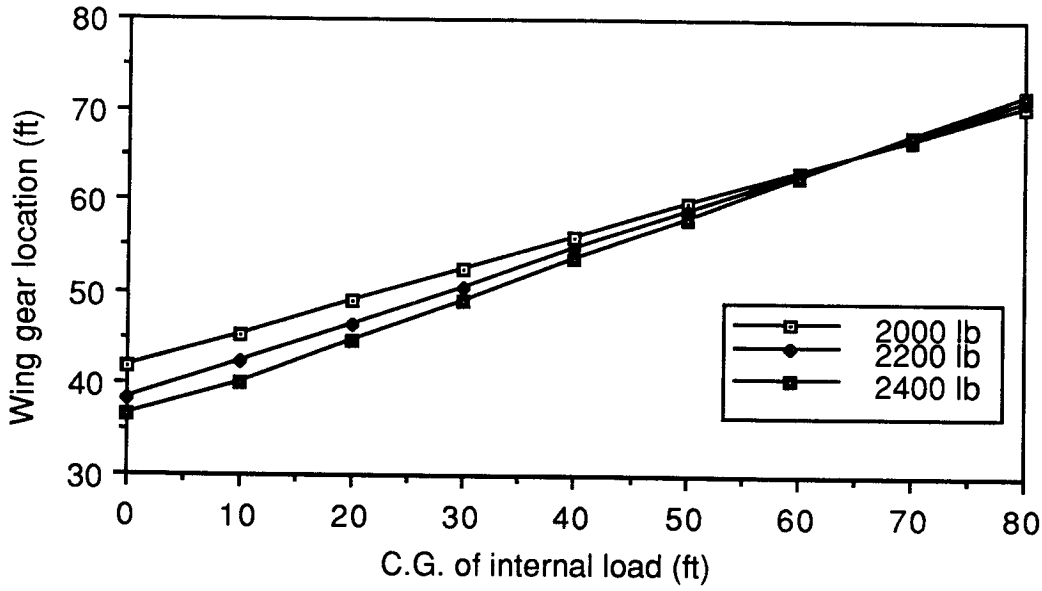

Figure 13.4.1 Wing gear location

wing gear, 120 ft, was not ideal for the specified taxiing of 90 ft, the wing gear will still fit the 150 ft required runway width. A solution to taxiing would be to have the aircraft towed to and from the runway. The wing gear each have a strut length of approximately 5 ft, utilizing an oleo-

pneumatic shock absorber with a stroke of 1.12 ft as do the main and nose gear. Since the purpose of the wing gear was to support the wing in the event of bending when under the influence of ground loads, the tires were sized to carry the engine in addition to auxiliary equipment located along the wing span. As a result, a tire size of 8.5 - 10 with a maximum load of 4,400 lb was used.

The main gear was designed to carry 80% of the total takeoff weight. Two tires were used to support the 80% load in case of tire malfunctions. Thus, a tire size of 12.50-16 with a maximum load of 12,800 lb was used. The main gear was located 15 ft aft of the c.g., or 45 ft from the nose. With the aforementioned location and a strut length of 7 ft., a pitch angle of 10 degrees could be achieved for landing or takeoff.

The remaining 20% of the gross weight would be carried by the nose gear 5 ft from the nose. For reasons similar to the main gear, this 20% of the total aircraft load was divided between two tires resulting in a comparatively smaller tire size. In this case, the tire size of the nose gear was the same as the wing gear. This would limit the number of spare tires to two tire sizes. Like the main gear the strut length was 7 ft to allow clearance for the propeller blades.

Deployed landing gear is depicted in Figure 13.4.2. The doors of the landing gear are coupled. A larger door was used to structurally support the struts. As a result, this is depicted swinging open with the gear intact. Before these gears can be released, a shorter sliding door was employed to allow the tires passage.

The main gear was chosen to fall rearward, so that in the event of any level of hydraulic failure the gear may be deployed by aerodynamic forces.

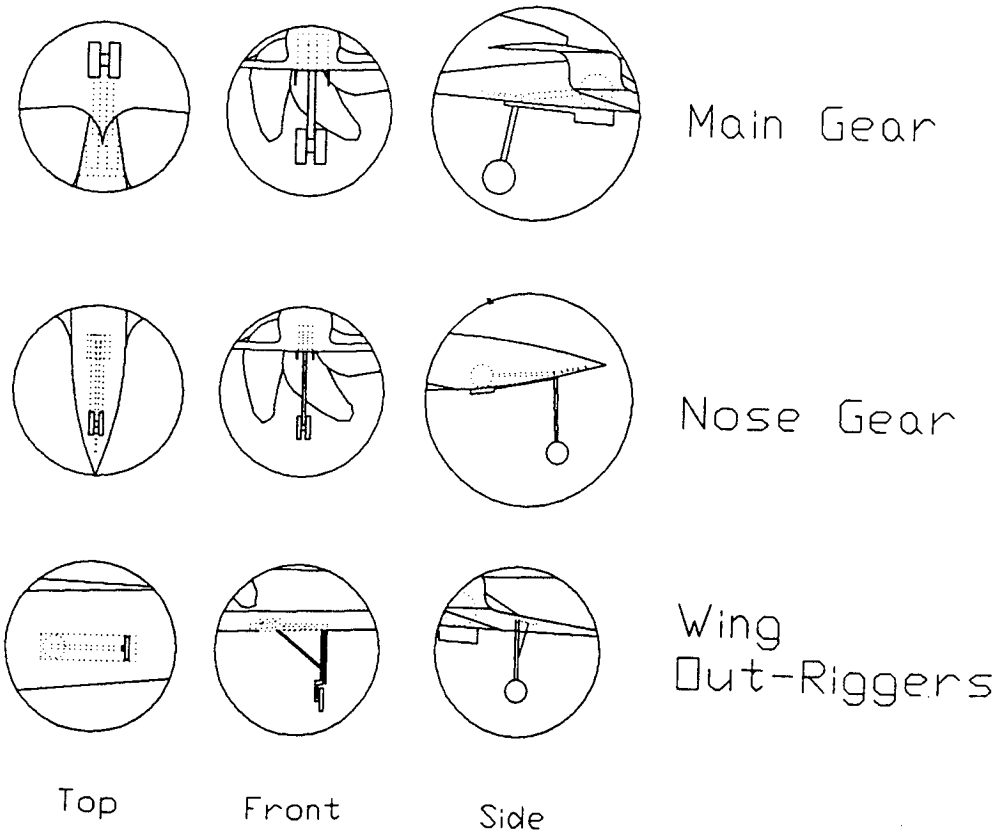

Figure 13.4.2 Landing gear detail

14.0 COST ANALYSIS

Cost estimation is a method specifically designed to forecast project cost and is used in industry. The methods take into account the cost of engineering, material, tooling, and designing factors. However, cost estimating is not limited to predicting project cost. Uses involve feasibility analysis of the product; determination of which process, method, or material is the best and least expensive; or quality control. The method used in determining the Life Cycle Cost (LCC) of the aircraft **SHARP** was obtained from Reference #1.

14.1 RESEARCH, DEVELOPMENT, TESTING & EVALUATION

The research, development, testing and evaluation (RDT&E) cost accounts for all costs incurred in phases 1, 2, and 3, which are planning and conceptual design, preliminary design and system integration, and detail design and development, respectively. The cost involved in this initial stage is $138,600,000 for one RDT&E aircraft.

14.2 ACQUISITION AND MANUFACTURING COSTS

In relation to the LCC, acquisition and manufacturing involves cost incurred during phase 4, manufacturing and acquisition. Since the program is funded by the government, the acquisition and manufacturing cost are equivalent. In determining the cost for this stage, it was assumed that only one other aircraft is to be manufactured. Thus, for the **SHARP** program a total of two planes, one manufactured and the RDT&E aircraft brought up to standard, are to be created for operational use. With this assumption, the method from Reference #1 is

not valid for small productions. However, it gives an idea for how much the program will cost. To create one more aircraft, it would cost an additional $34,000,000. An estimate for the unit price per airplane is $89,400,000.

14.3 OPERATIONAL COST

In estimating for this phase, the operating cost of military airplanes was used as a guide. On the LCC scale, operation cost represents phase 5, operation and support. Operation cost takes into account the costs of fuel, oil and lubricants, direct maintenance personnel, consumable materials in conjunction with maintenance, spare parts, depots, and miscellaneous items (i.e. technical data support and training data and equipment). Figure 14.3.1 shows the distribution of program operating cost with the total cost being $6,400,000 for a 5 year use and 180 flight hours per year.

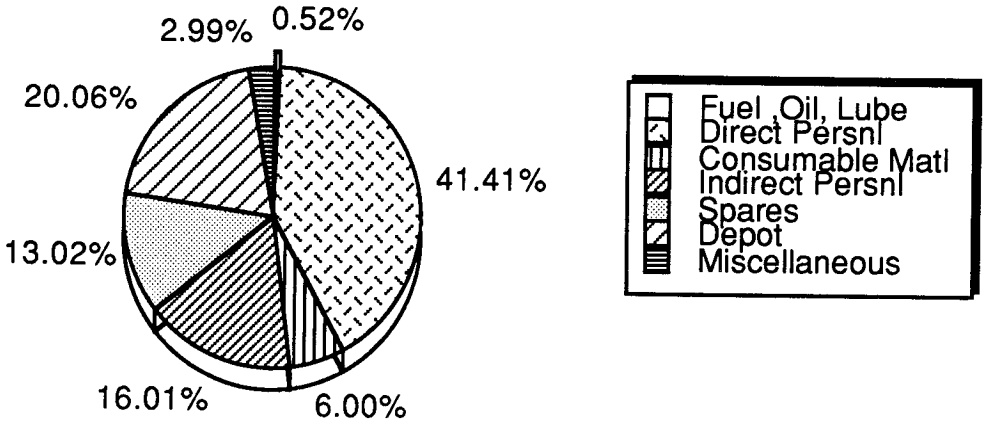

FIGURE 14.3.1 Distribution of operating cost over ten years

14.4 LIFE CYCLE COST

LCC takes into account all monies invested into the program from research and manufacturing to disposal. The cost of disposing the aircraft is $2,200,000. Thus, the life cycle cost of the **SHARP** aircraft over a 10 year period and 360 hours of flight time is $221,600,000. If only a 5 year period and 180 hours of flight is preferred, then LCC is $181,000,000 and the disposal cost becomes 1% of LCC.

14.5 COST-PER-POUND

The dollar values obtained from Reference #1 were high due to the inability of the method to account for low aircraft production programs. The more airplanes produced, the lower the cost per aircraft. However, with a cost-per-pound method, the cost for **SHARP** becomes $2,700,000 per airplane (assuming a 2 airplane production). The rate of $89.70 was obtained by taking the average cost per pound of several aircraft types.

15.0 MANUFACTURING

It is desired to have the **SHARP** aircraft operational by the year 2000 or earlier. Proposed GANTT and Pert charts are shown in Figures 15.0.1 and 15.0.2 to meet this requirement. Assuming proposal selection and finalization near the beginning of 1992, three plus years will be spent on technology confirmation and prototype development followed by a year and a half of testing and evaluation. This will allow production to begin a the start of 1997. The production of two operational aircraft is expected to take two and a half years. The production schedule assumes simultaneous manufacture of each individual component of the aircraft. Fuselage joining will take place one year into production followed by wing and empennage mounting and propulsion system integration. After final assembly, one half year is allowed for final testing and assembly. The extended periods of time for development and testing are required due to the high composite nature of the aircrafts' construction. Production periods have also been extended to allow for tooling, layup, and curing times for the composite components.

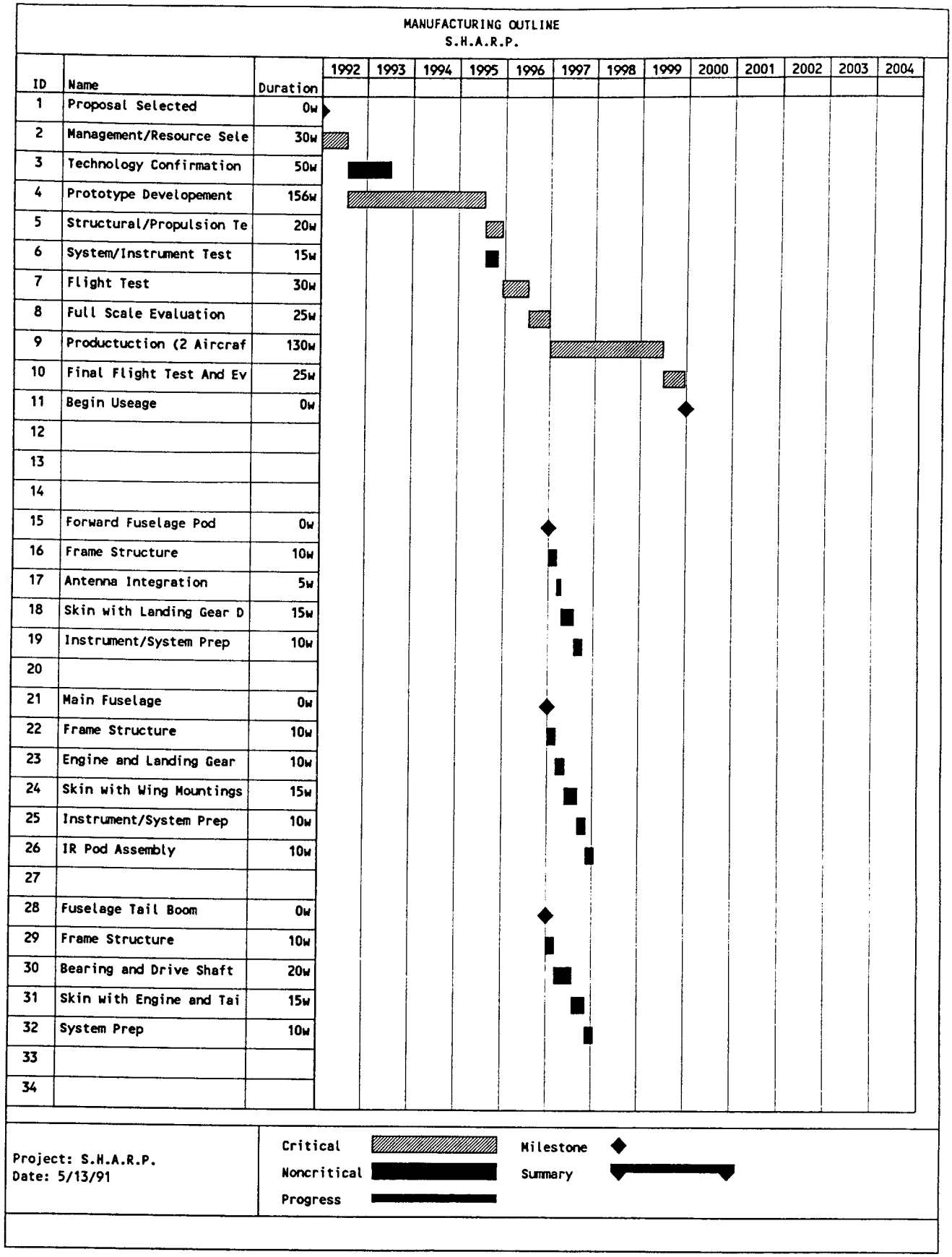

Figure 15.0.1 GANTT chart for the **SHARP** program

MANUFACTURING OUTLINE
S.H.A.R.P.

ID	Name	Duration
35	Empenage	0w
36	Tail Frame Structures	12w
37	Control Mechanics	15w
38	Skins and LE Reinforceme	20w
39	Vertical-Horizontal Tail	5w
40	System Prep	10w
41		
42	Wings	0w
43	Frame Structure	20w
44	Control Mechanics	10w
45	Antenna Integration	6w
46	Fuel System and Cells	15w
47	Instrument Compartments	10w
48	Engine Mounts and Out R	15w
49	Skin with LE Reinforceme	15w
50	Instrument and System Pr	10w
51		
52	Engine	0w
53	Engine Construction	40w
54	Inlet and Exaust Integra	4w
55	Fuel and Controls Prep	6w
56		
57	Propeller	0w
58	Main Spar and Filler	4w
59	Skin with LE Reinforceme	4w
60	Variable Pitch Assembly	10w
61	Propeller-Engine Integra	5w
62		
63		
64		
65		
66		
67		
68		

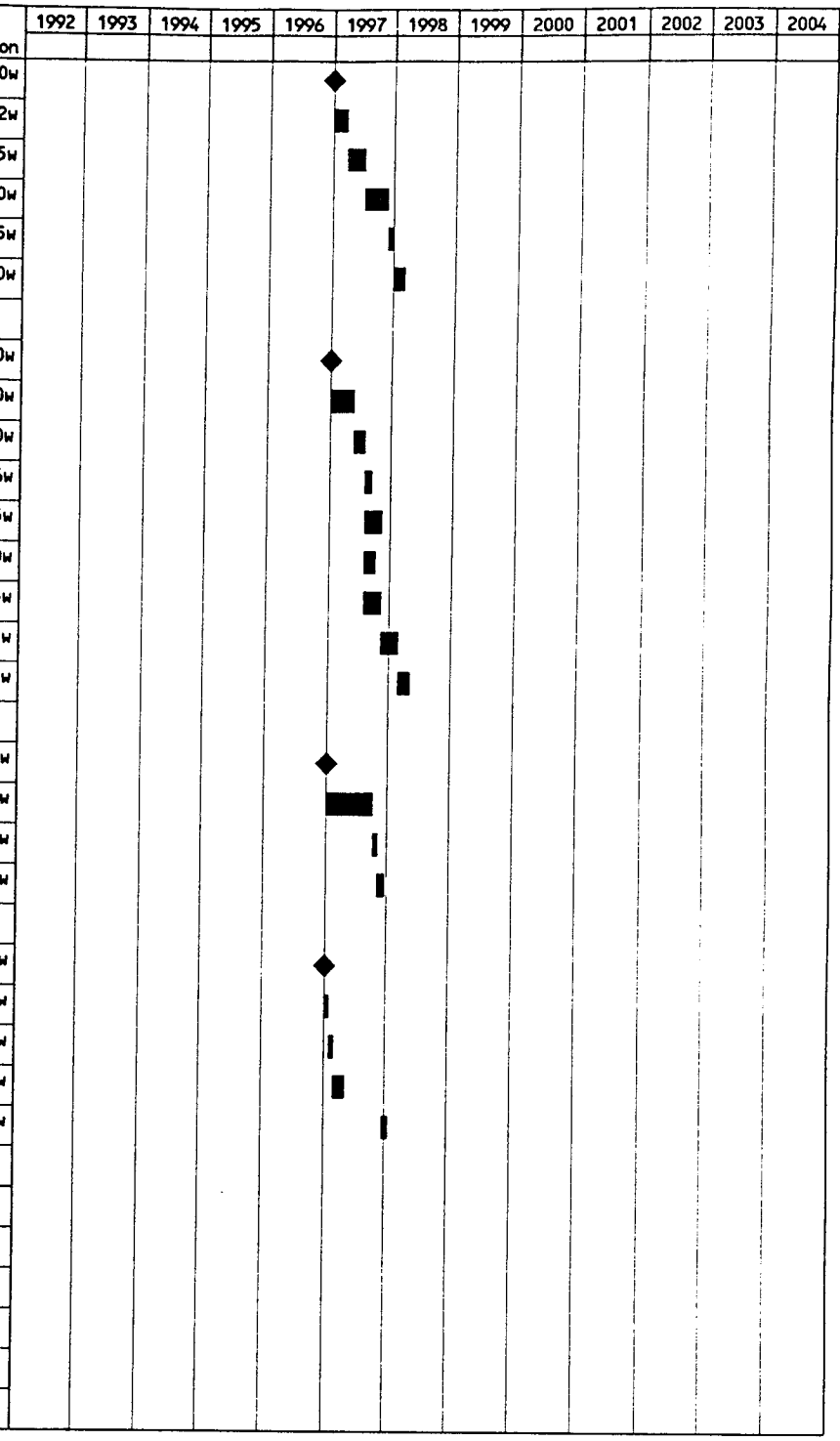

Project: S.H.A.R.P.
Date: 5/13/91

Critical
Noncritical
Progress
Milestone
Summary

MANUFACTURING OUTLINE
S.H.A.R.P.

ID	Name	Duration
69	Fuselage Mating	6w
70		
71	Main and Nose Landing ge	15w
72	Instrument/System Integr	5w
73	Auxilary Engine Inlet	5w
74	Additions to Fuselage	10w
75		
76	Fuselage-Wing Mating	12w
77	Fuselage-Empenage Mating	7w
78	Engine/Propeller Mountin	10w
79		
80	Engine Nacell Installati	10w
81	Instrument Installation	3w
82	Final Assembly	10w
83	Final Inspection	10w

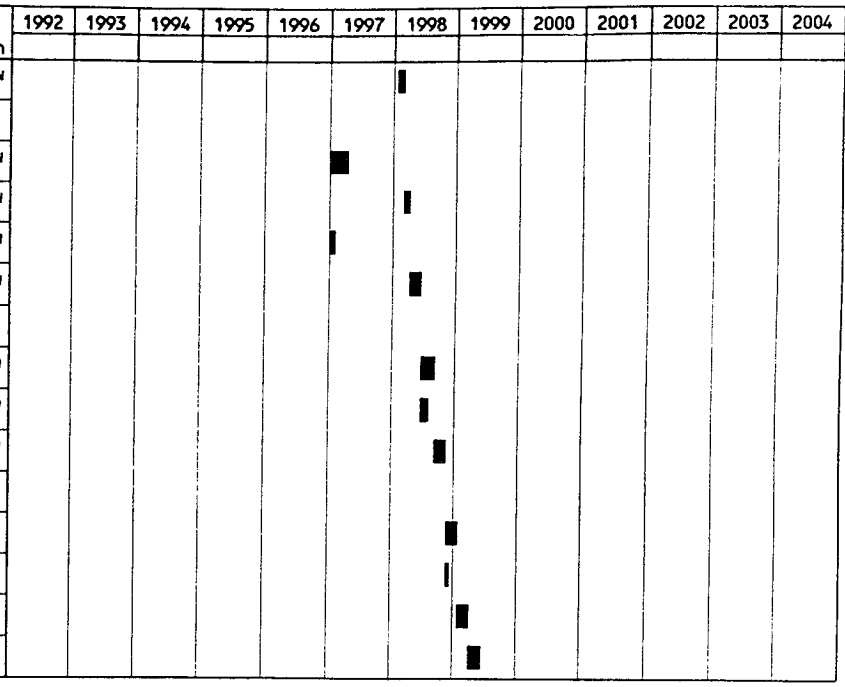

Project: S.H.A.R.P.
Date: 5/13/91

Critical
Noncritical
Progress
Milestone
Summary

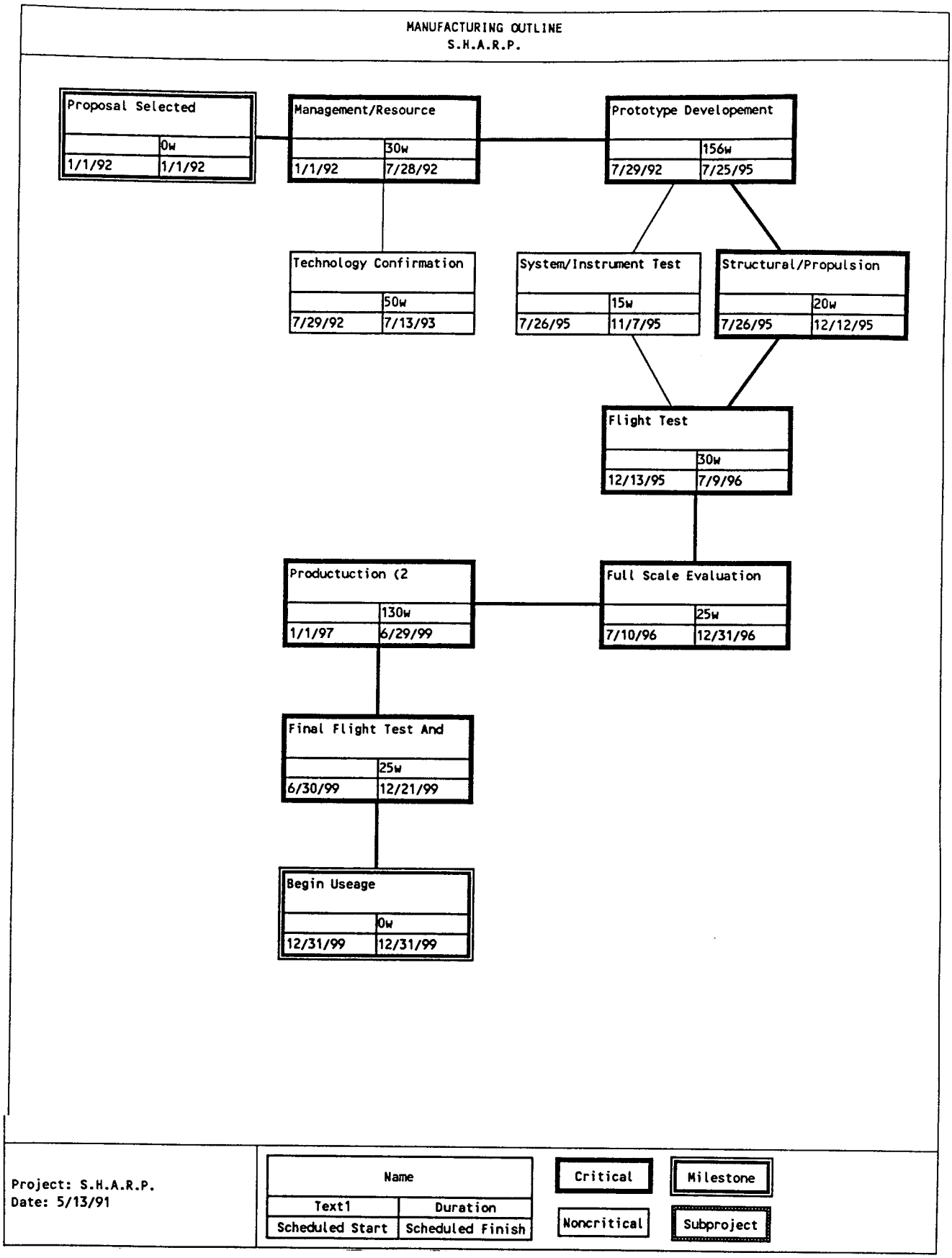

Figure 15.0.2 Pert chart for the **SHARP** program

16.0 OPERATIONS

Because the design of the **SHARP** stresses the notion of self-containment, there will be no need to transport the aircraft to and from operational sites except under its own power and control. SHARP's range and minimal runway requirements allows almost any site around the world to be accessible and its simple, modular systems with easy-access panels provide ease and speed in maintenance and service.

Because of its minimal needs, **SHARP** requires only a minor staffing of operators and flight crew. Preliminary studies indicate that a flight crew of 20 personnel per site, including a Flight Director, would provide adequate. This estimate is made on a per-aircraft basis and does not include scientific crew. Take-off and landing sites should include the following minimal support:

- A ground control center with at least one redundant control system. The station can be located in a van, a mobile trailer, or a more permanent structure such as a building. The location of the control center should be within visual range of the take-off and landing strip to allow human control if the aircraft's on-board autopilot systems should fail.

- Provisions for fuel storage and transfer. A fuel trailer containing aviation gasoline will be the most efficient means of filling and draining the on-board fuel tanks as well as containing the fuel during periods of inactivity. Fire-safety provisions will be needed as well.

- Ground servicing lifters, carts and tools as well as diagnostic equipment to insure flight computer and engine efficiency and reliability.

- A tow vehicle to maneuver the aircraft into and out of storage. The vans used to transport the ground control center equipment should prove satisfactory.

16.1 OPERATING SITES

A typical series of missions of **SHARP** can follow one another sequentially with refueling and service at each intermediate landing point. A typical series could be as follows (full fuel and instrumentation, unless noted):

- Moffett Field, California (37°N) to Puerto Montt, Chile (41°S) at 100,000 feet cruise altitude.
- Partial fuel for a short transfer excursion from Puerto Montt (41°S) to Punta Arenas, Chile (53°S).
- Punta Arenas, Chile (53°S) to South Pole, Antarctica (90°S) and back to Punta Arenas,Chile at 70,000 feet.
- Punta Arenas, Chile (53°S) to South Pole, Antarctica (90°S) and back to Punta Arenas, Chile at 100,000 feet.

It is assumed that these designated sites are as unpopulated as possible and that they contain minimal airport facilities.

16.2 PERSONNEL

Crew site requirements are estimated at twenty, consisting of the following:

- Flight Director, in charge of the overall management scheme.
- Pilots (3), who are aware and knowledgeable of the aircraft and its systems. They will operate in shifts monitoring the aircraft's flight and performance.
- Engineers (4), who will interact between the main engineering team and the field team. Areas of specialty will include Airframe, Propulsions Systems, Avionics and Flight Control.
- Technicians (12), specializing in all major areas of the aircraft configuration.

16.3 AIR TRAFFIC CONTROL

Because of the absence of Federal Air Regulations pertaining to the design, certification or operation of unmanned, military aircraft, issues pertaining to the flying over populated areas will have to be dealt with as they arise. Since many of the proposed missions will take place over the water or other unpopulated areas, this is not a major issue. For safety, however, the following practices will be adopted in **SHARP**:

- Dual, redundant radio frequencies for command and control. If interference on one frequency occurs, the aircraft will shift to the other, If it should experience trouble with both channels, on-board flight logic will establish control on a pre-set heading until communication is again established.

- A mode C transponder, which emits a coded signal identifying the aircraft and its altitude when interrogated by an FAA air surveillance radar or by another aircraft. The use of Mode C will allow the operation of the TCAS collision avoidance system now being developed by the FAA.

- A flight termination device, comprised of a mortar-launched parachute activated either on a.) ground command, by a coded signal on a completely separate radio frequency, or b.) internal logic in the flight control computer, which determines that the aircraft is out of control, has experienced a structural failure, or has exceeded a specified velocity and cannot be recovered.

- Strobe lights and radar reflectors (consisting of the cooling surfaces on the wings) to enhance the general visibility of the platform.

REFERENCES

#1. Roskam, J., Airplane Design Series, University of Kansas, 1985.

#2. Raymer, D.P., Aircraft Design: A conceptual Approach, AIAA Inc., 1989.

#3. Stinton, D., The Design of the Aeroplane, Van Nostrand Reinhold Co., 1983.

#4. Olsen, B. and Selenberg, S., Optimization of Biplane Aerodynamics, 1984.

#5. Nelson, R., "The Influence of Airfoil Roughness on the Performance of Flight Vehicles at Low Reynolds Numbers," AIAA-84-0540.

#6. Mil-F-8785C, Military Specification: Flying Qualities of Piloted Airplanes, November 5, 1980.

#7. Blackelock, J.H., Automatic Control of Aircraft and Missiles, John Wiley & Sons, Inc., 1965.

BIBLIOGRAPHY

Abbott, I., and Von Doenhoff, A., Theory of Wing Sections, Dover Publications, New York, 1959.

AFDA, Professor Paul Lord, Software Package, Cal Poly Pomona.

Aircraft Maintenance and Repair, McGraw-Hill Book Company, Inc., New York, 1955.

Ashmead, Gordon B., Aircraft Production Methods, Chilton Company, Philadelphia, 1956.

Baullinger, N., and Page, V., AIAA 89-2014, High Altitude Long Endurance (HALE) RPV, AIAA/AHS/ASEE Aircraft Design, Systems and Operations Conference, July - August 1989.

Bertin, J., and Smith, M., Aerodynamics for Engineers, Prentice Hall, New Jersey, 1989.

Bojkov, R. D., and Fabian, P., Ozone in the Atmosphere, A. Deepak Publishing, 1989.

Brimm, Daniel J., and Boggess, H. Edward, Aircraft Maintenance, Fourth Ed., Pitman Publishing Corporation, New York, 1940.

Corning, Gerald, Supersonic and Subsonic Airplane Design, Edwards Brothers, Inc., Ann Arbor, 1953.

Cost Effectiveness - Principles and Applications to Aerospace Systems, Vol. 5, AIAA Lecture Series, 1966.

Currey, Norman S., Aircraft Landing Gear Design: Principles and Practices, American Institute of Aeronautics and Astronautics, Inc., Washington D.C., 1988.

Gatzen, Bernard S., Advanced Turboprop Propulsion Technology, United Technologies Hamilton Standard, May 1982.

Gatzen, Bernard S., Potential and Technology Readiness, Hamilton Standard, Dec. 1985.

BIBLIOGRAPHY (Continued)

"Global Stratospheric Change: Requirements for a Very-High-Altitude Aircraft for Atmospheric Research," NASA Report #NASA CP-10041, Nov. 1989.

Higdon, A. et al., Mechanics of Materials, John Wiley & Sons Inc., 1985.

"High Altitude Atmospheric Research Platform (HAARP) Development, Lockheed Aeronautics Systems, Feb. 1990.

Horne, Douglas F., Aircraft Production Technology, Cambridge University Press, Cambridge, 1986.

International Ozone Commission, Atmospheric Ozone, D. Riedel Publishing Co., 1985.

Jarman, David L., Design, Engineering, and Manufacturing Processes at Douglas Aircraft, Abstract, California State University of Long Beach, August 1988.

King, Frank H., Aviation Maintenance Management, Southern Illinois University Press, Carbondale, 1986.

The Leading Edge, General Electric Company, Fall 1986.

Ludema, Kenneth C., Caddell, Robert M., and Atkins, Anthony G., Manufacturing Engineering, Economics and Processes, Prentice-Hall, Inc., Englewood Cliffs, 1987.

McCormick, E.J., and Sanders, M.S., Human Factors in Engineering and Design, McGraw Hill, New York, 1982.

Nelson, Robert C., Flight Stability and Automatic Control, McGraw-Hill Book Company, New York, 1989.

Ostwald, Phillip F., ed., Manufacturing Cost Estimating, Society of Manufacturing Engineers, Dearborn, 1980.

Russell, P., Science Justification and Requirements, HQ Presentation, Sep. 1988.

BIBLIOGRAPHY (Continued)

Shevell, R., Fundamentals of Flight, Prentice Hall, New Jersey, 1989.

STADERP, Professor Paul Lord, Software Package, Cal Poly Pomona.

Stewart, Rodney D., Cost Estimating, John Wiley & Sons, New York, 1982.